



(12)

## EUROPEAN PATENT APPLICATION

(43) Date of publication:  
22.04.1998 Bulletin 1998/17

(51) Int. Cl.<sup>6</sup>: H04L 27/26

(21) Application number: 97117972.6

(22) Date of filing: 16.10.1997

(84) Designated Contracting States:  
AT BE CH DE DK ES FI FR GB GR IE IT LI LU MC  
NL PT SE

Designated Extension States:  
AL LT LV RO SI

(30) Priority: 18.10.1996 JP 275968/96

(71) Applicant:  
Alpine Electronics, Inc.  
Tokyo 141 (JP)

(72) Inventor: Nemoto, Hiroyuki  
Iwaki-city, Fukushima (JP)

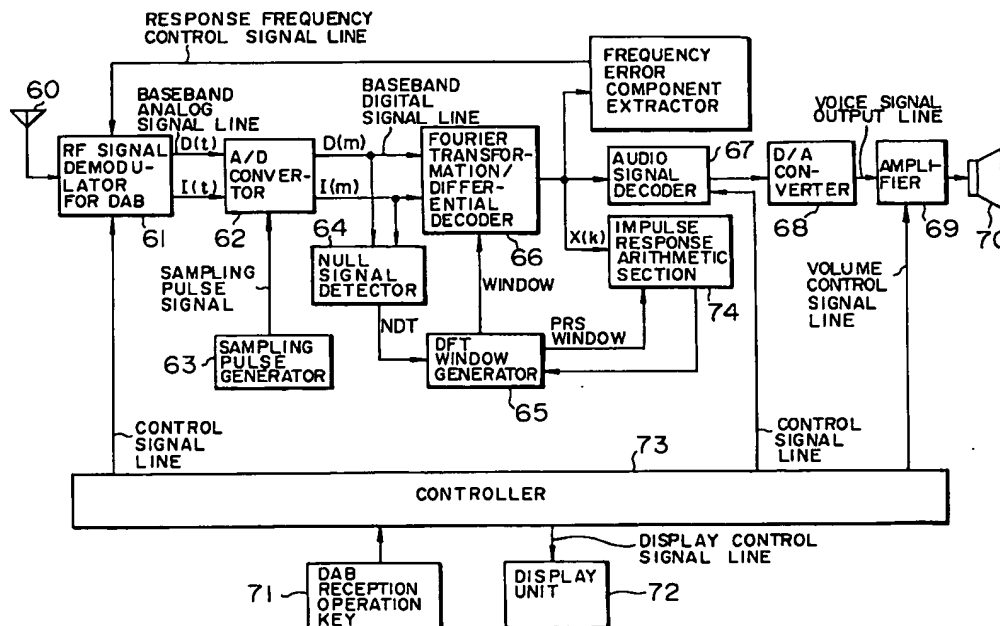
(74) Representative: Hirsch, Peter  
Klunker Schmitt-Nilson Hirsch  
Winzererstrasse 106  
80797 München (DE)

## (54) Symbol synchronization in a DAB receiver

(57) A DFT window generator 65 sequentially shifts the position of a window having a guard interval width  $\Delta$  and calculates the energy of an impulse response in a window at respective positions to obtain a window position where the maximum energy can be obtained, and

the window position where the maximum energy can be obtained is set as the start edge position of the DFT window.

FIG.10



## Description

## BACKGROUND OF THE INVENTION

## 1. Field of the Invention

The present invention relates a receiver in a digital audio broadcast (Digital Audio Broadcast: DAB) and, more particularly, to a receiver in digital audio broadcast in which even if a multipath is generated, a DFT window for giving a Fourier transformation execution timing can be set at a position which is not interfered from an adjacent symbol or minimally interfered by the adjacent symbol.

## 2. Description of the Related Art

Digital audio broadcast (DAB) in which audio signals are converted into digital signals to obtain serial data, the serial data are divided into sets each consisting of  $2N$  digital data, the  $2N$  digital data are divided into  $N$  groups each having two bits,  $N$  carriers having different frequencies depending on combinations of 1 and 0 of each two bits are 4-phase-PSK-modulated, the modulated signals are frequency-multiplexed to be sent from a transmission station, the frequency-multiplexed phase-modulated signal is received by a receiver and demodulated to be an audio output is proposed. The DAB is being studied for practical use in Europe and the like.

In this DAB scheme, in order to reduce influence of selectivity fading, pieces of information are divided in parallel, and modulation is performed by using a plurality of carriers. As a result, even if any carrier receives fading, influence is reduced as a whole. Basically, the DAB scheme is a frequency division multiplex (FDM: Frequency Division Multiplex) scheme. In a simple FDM, an interval between carriers must be sufficiently large to avoid spectra from overlapping, and good frequency use efficiency cannot be obtained. For this reason, an OFDM (Orthogonal Frequency Division Multiplex) scheme is proposed. In this OFDM, carriers are arranged to satisfy orthogonal conditions and to allow spectra to overlap, good frequency use efficiency can be obtained, and IDFT (Inverse Discrete Fourier Transform) and DFT (Discrete Fourier Transform) operations can be used in a modulator and a demodulator, thereby advantageously obtaining very simple hardware.

## (a) Principle of Digital Audio Broadcast by OFDM Scheme

FIG. 13 is a view showing the theoretical arrangement of a transmitter for digital audio broadcast. Reference numeral 1 denotes a serial/parallel converter (S/P converter) for converting serial data  $d(n)$  ( $a(0)$ ,  $b(0)$ ,  $a(1)$ ,  $b(1)$ , ...) input at a transmission rate  $f_s (= 2/\Delta t)$  into  $2N$ -bit parallel data;  $2_0$  to  $2_{N-1}$ ,  $N$  carrier multiplying sections for dividing the  $(2 \times N)$ -bit parallel data into  $N$  groups  $a(0)$ ,  $b(0)$ ;  $a(1)$ ,  $b(1)$ ; ...;  $a(N-1)$ ,  $b(N-1)$  each having two bits, multiplying the first bits  $a(0)$ ,  $a(1)$ , ...,  $a(N-1)$  of the groups by carriers  $(\cos \omega_n t)$  having frequencies  $f_0$  to  $f_{N-1}$ , and multiplying the second bits  $b(0)$ ,  $b(1)$ , ...,  $b(N-1)$  by carriers  $(-\sin \omega_n t)$  having frequencies  $f_0$  to  $f_{N-1}$ ; and 3, a frequency multiplexer (MUX) for synthesizing output signals  $a(n)\cos \omega_n t$  and  $-b(n)\sin \omega_n t$  ( $n = 0$  to  $N-1$ ) from the carrier multiplying sections of the respective groups and frequency-multiplexing the synthesized signal to send a signal  $D(t)$ .

When output signals from the carrier multiplying sections of the respective groups are synthesized by the frequency multiplexer 3, the carriers having frequencies  $f_0$  to  $f_{N-1}$  are 4-phase-PSK-modulated by combinations of 1 and 0 of two bits of each group. The output  $D(t)$  from the frequency multiplexer 3 is given by:

$$D(t) = \sum \{a(n)\cos \omega_n t - b(n)\sin \omega_n t\} \quad (n = 0 \text{ to } N-1)$$

Note that, when the frequency interval of carriers is represented by  $\Delta f$ , the  $(n+1)$ th carrier frequency  $f_n$  is given by:

$$f_n = f_0 + n\Delta f$$

When a transmission time of 2-bit data is represented by  $\Delta t$  (transmission rate  $f_s = 2/\Delta t$ ), the frequency interval  $\Delta f$  is given by:

$$\Delta f = 1/N\Delta t$$

FIG. 14 is a view for explaining the function of the frequency multiplexer 3.  $N$  carriers  $f_0$  to  $f_{N-1}$  having intervals  $\Delta f$  are 4 $\phi$ -PSK-modulated by data  $a(0)$ ,  $b(0)$ ;  $a(1)$ ,  $b(1)$ ; ...;  $a(N-1)$ ,  $b(N-1)$  of  $N$  2-bit groups, and the modulated signals are frequency-multiplexed to be transmitted. FIG. 15 is a view for explaining a symbol. One symbol consists of  $2 \times N$  bits. When the time length of one symbol is represented by  $T_s$ , the following equations can be obtained:

$$T_s = N\Delta t$$

$$\Delta f = 1/T_s$$

5 Every symbol ( $2 \times N$  bits) is subjected to  $4\phi$ PSK modulation, and the modulated signals are frequency-multiplexed, thereby sequentially transmitting frequency multiplication signals  $D(t)$ .

FIG. 16 is a view showing a theoretical arrangement of a receiver for digital audio broadcast. Reference numerals  $4_0$  to  $4_{N-1}$  denote  $N$  carrier multiplying sections for multiplying the received signal  $D(t)$  by carriers ( $\cos \omega_n t$ ,  $-\sin \omega_n t$ ,  $n = 0$  to  $N-1$ ) having frequencies  $f_0$  to  $f_{N-1}$ ;  $5_0$  to  $5_{N-1}$ , integrators for integrating outputs from the multiplying sections to demodulate data; and 6, a parallel/serial converter (P/S converter) for converting  $2 \times N$ -bit parallel data into serial data.

The integrators  $5_0$  to  $5_{N-1}$  perform the following arithmetic operation to an input signal  $D(t)$ :

$$\begin{aligned} \text{[Equation 1]} \quad \int_0^{T_s} D(t) \cos(\omega_n t) dt &= \frac{N\Delta t}{2} a(m) = \frac{T_s}{2} a(m) \\ \therefore a(m) &= \frac{2}{T_s} \int_0^{T_s} D(t) \cos \omega_n t dt \end{aligned}$$

to demodulate data  $a(0)$ ,  $b(0)$ ;  $a(1)$ ,  $b(1)$ ; ...;  $a(N-1)$ ,  $b(N-1)$ .

(b) OFDM Modulation Scheme using DFT

In order to generate a baseband signal  $D(t)$  of OFDM,  $N$   $4\phi$ PSK modulators are required. In addition,  $N$   $4\phi$ PSK demodulators are required to demodulate the baseband signal  $D(t)$ . When the number  $N$  is large, this scheme is not in practical use. Therefore, a method of simply performing modulation/demodulation by using DFT will be described below.

(b-1) Arrangement of Modulator

A baseband signal of OFDM is expressed by the following equation:  
[Equation 2]

$$D(t) = \sum_{k=0}^{N-1} \{a(k) \cos \omega_k t - b(k) \sin \omega_k t\} \quad (1)$$

When  $d(k) = a(k) + jb(k)$  is established, Equation (1) is expressed as follows:  
[Equation 3]

$$\begin{aligned} D(t) &= R[D^*(t)] \\ &= R\left[\sum_{k=0}^{N-1} d(k) e^{j\omega_k t}\right] \end{aligned} \quad (2)$$

where  $*$  means a complex number, and  $R[\ ]$  represents the real-number part of  $\[ \]$ .

Since the following equation is established:

[Equation 4]

$$\begin{aligned}
D^*(t) &= \sum_{k=0}^{N-1} d(k) e^{j\omega_k t} \\
&= \sum_{k=0}^{N-1} [(a_k + jb_k) \cos \omega_k t + j(a_k + jb_k) \sin \omega_k t] \\
&= \sum_{k=0}^{N-1} (a_k \cos \omega_k t - b_k \sin \omega_k t) + j(a_k \sin \omega_k t + b_k \cos \omega_k t) \\
&= D(t) + jI(t)
\end{aligned} \tag{3}$$

it is apparent from Equation (3) that  $D(t)$  is expressed by Equation (2). In Equation (2), when  $t = m\Delta t$  is established, [Equation 5]

$$\begin{aligned}
D(m) &= R \left[ \sum_{k=0}^{N-1} d(k) e^{j\omega_k \cdot m \cdot \Delta t} \right] \\
&= R \left[ \sum_{k=0}^{N-1} d(k) e^{j2\pi \frac{km}{N}} \right]
\end{aligned} \tag{4}$$

where it must receive attention that  $D(m)$  is the real-number part of IDFT (Inverse Discrete Fourier Transform) of  $d(k)$ . When  $D(m)$  is output as  $D(0), D(1), \dots, D(N-1)$  for each  $\Delta t$ ,  $D(m)$  is expressed as shown in FIG. 17. This signal must be obtained by sampling Equation (2) for each  $\Delta t$ . Therefore, when the signal passes through an ideal filter having the frequency characteristic shown in FIG. 18A and the impulse characteristic shown in FIG. 18B, the same equation as Equation (2) can be obtained.

As is apparent from the above description, in the modulator, IDFT is performed to input data  $d(k)$  (complex), and the real-number parts  $D(0)$  to  $D(N-1)$  are output for each  $\Delta t$  and are caused to pass through the ideal filter, thereby obtaining a modulation-wave (baseband signal). FIG. 19 is a view showing the arrangement of a main part of a transmitter constituted while giving attention to this point. Reference numeral 11 denotes an IDFT section for performing inverse discrete Fourier transform to input data  $d(k)$  which is expressed as complex numbers by data  $a(k), b(k)$  ( $k = 0$  to  $N$ ) of  $N$  groups each having two bits; 12a, a DA converter for converting a real-number part output from the IDFT section into an analog signal; 13a, an ideal filter; 14a, a multiplying section for multiplying an ideal filter output  $D(t)$  by  $\cos \omega t$  to perform frequency conversion.

#### (b-2) Arrangement of Demodulator

When only  $D(t)$  is obtained by received frequency conversion, original information cannot be extracted without sampling  $2N$  points. This is because  $D(t)$  consists of the real-number part of IDFT at  $N$  points. This is apparent from a sampling theorem as shown in FIGS. 20A and 20B. According to the sampling theorem, a signal in a band  $N \cdot \Delta f$  must be sampled at a frequency of  $1/(2 \cdot N \cdot \Delta f)$ . Since the following equation is established:

$$1/(2 \cdot N \cdot \Delta f) = \Delta t/2,$$

the signal must be sampled at an interval of  $\Delta t/2$  but an interval of  $\Delta t$ . For this reason, sampling at  $2N$  points must be performed in  $T_s$  zone ( $N \cdot \Delta t$ ).

However, when a real-number part  $D(t)$  and an imaginary-number part  $I(t)$  are obtained, an original signal can be extracted by sampling at  $N$  points as in the following description.

A complex baseband signal obtained after received frequency conversion is expressed in Equation (5). [Equation 6]

$$Y^*(t) = \hat{D}(t) + j\hat{I}(t) \tag{5}$$

The right-hand real-number part and the right-hand imaginary-number part are obtained by deforming  $D(t)$  and  $I(t)$  by the transmission path and noise. When an ideal transmission path is used, the right-hand real-number part and the right-hand imaginary-number part are equal to  $D(t)$  and  $I(t)$ , respectively.

[Equation 7]

$$\begin{aligned}
Y^*(t) &= \sum_{k=0}^{N-1} (\hat{a}_k \cos 2\pi f_k t + \hat{b}_k \sin 2\pi f_k t) + j(\hat{a}_k \sin 2\pi f_k t + \hat{b}_k \cos 2\pi f_k t) \\
&= \sum_{k=0}^{N-1} (\hat{a}_k + j\hat{b}_k) \cos 2\pi f_k t + j(\hat{a}_k + j\hat{b}_k) \sin 2\pi f_k t \\
&= \sum_{k=0}^{N-1} \hat{d}(k) e^{j\omega_k t}
\end{aligned} \tag{6}$$

Assume that Equation (6) is sampled by  $m\Delta t$  ( $m = 0, 1, 2, \dots, N-1$ ). In this case, when the following equation is established:  
[Equation 8]

$$\begin{aligned}
Y^*(m) &= \sum_{k=0}^{N-1} \hat{d}(k) e^{j\omega_k m \Delta t} \\
&= \sum_{k=0}^{N-1} \hat{d}(k) e^{j2\pi \frac{km}{N}} \\
y^*(m) &= \frac{Y^*(m)}{N}
\end{aligned} \tag{7}$$

Equation (7) can be expressed by the following equation:  
[Equation 9]

$$y^*(m) = \frac{1}{N} \sum_{k=0}^{N-1} \hat{d}(k) e^{j2\pi \frac{km}{N}} \tag{8}$$

Therefore,  $\hat{d}(k)$  is obtained by Equation (8) as described follows.  
[Equation 10]

$$\hat{d}(k) = \sum_{m=0}^{N-1} y^*(m) e^{-j2\pi \frac{km}{N}} \tag{9}$$

According to this equation, an estimation value of the original signal  $\hat{d}(k)$  is obtained. As only a reference, the relational expression between DFT and IDFT is given by the following equation:  
[Equation 11]

$$\begin{aligned}
X_k &= \sum_{\pi=0}^{N-1} x_\pi e^{-j2\pi \frac{k\pi}{N}} \\
x_\pi &= \frac{1}{N} \sum_{k=0}^{N-1} X_k e^{j2\pi \frac{\pi k}{N}}
\end{aligned} \tag{10}$$

As described above, a complex baseband signal obtained by frequency-converting a received signal  $S(t)$  is converted into a digital signal through a low-pass filter. When the digital signal is subjected to DFT by the DFT section, the estimation value of the original signal  $\hat{d}(k)$  is obtained. FIG. 21 is a view showing the arrangement of a main part of a receiver constituted while giving attention to this point. Reference numeral denotes a frequency converter; 16a and 16b, low-pass filters; 17a and 17b, A/D converters; and 18, a DFT section.

## (c) Frequency Conversion on Transmission Side

An orthogonal balance modulation scheme using  $D(t)$  and  $I(t)$  is the same as a frequency conversion scheme used in an SSB scheme as shown in FIG. 22. Referring to FIG. 22, reference numeral 11 denotes an IDFT section; 12a and 12b, AD converters; 13a and 13, low-pass filters; and 14, a frequency converter. The frequency converter 14 is constituted by multiplying sections 14a and 14b for multiplying  $\cos \omega_c t$  and  $\sin \omega_c t$  and a hybrid circuit 14c for synthesizing outputs from the multiplying sections to output a synthesized signal.

An output signal  $S(t)$  from the frequency converter 14 is given by the following equation:  
[Equation 12]

$$\begin{aligned}
 s(t) &= D(t) \cos \omega_c t + I(t) \sin \omega_c t \\
 &= \sum_{k=0}^{N-1} (a_k \cos 2\pi f_k t - b_k \sin 2\pi f_k t) \cos 2\pi f_c t + \sum_{k=0}^{N-1} (a_k \sin 2\pi f_k t + b_k \cos 2\pi f_k t) \times (-\sin 2\pi f_c t) \\
 &= \sum_{k=0}^{N-1} (a_k \cos 2\pi (f_k + f_c) t - b_k \sin 2\pi (f_k + f_c) t)
 \end{aligned}
 \tag{11}$$

The signal  $S(t)$  does not include a lower sideband. Therefore, in this scheme, a band which is 1/2 the band in a both-sideband scheme can be obtained, and transmission efficiency is improved.

## (d) Frequency Conversion Scheme on Reception Side

FIG. 23 is a view showing the arrangement of an orthogonal frequency converter using  $\cos \omega_c t$  and  $\sin \omega_c t$ . Reference numeral 15a denotes an adder (not actually exist) for adding a noise signal  $n(t)$  expressed by the following equation:

$$n(t) = n_c(t) \cos 2\pi (f_c + f_k) t - n_s(t) \sin 2\pi (f_c + f_k) t$$

to a received signal  $s(t)$  (see Equation (11)) to output a signal  $r(t)$ ; 15b, a bandpass filter; and 15c and 15d, multiplying sections for multiplying a bandpass filter output by  $\cos \omega_c t$  and  $-\sin \omega_c t$ . In an ideal transmission path which is free from amplitude attenuation, noise, and phase delay,  $r(t) = s(t)$  is established. The following description is on the assumption that  $r(t) = s(t)$  is established. Output signals  $D'(t)$  and  $I'(t)$  from the orthogonal frequency converter are expressed by the following equations, respectively:

[Equation 13]

$$\begin{aligned}
 D'(t) &= \sum_{k=0}^{N-1} [a_k \cos 2\pi (f_c + f_k) t - b_k \sin 2\pi (f_c + f_k) t] \cos 2\pi f_c t \\
 &= \frac{1}{2} \sum_{k=0}^{N-1} [a_k \cos 2\pi f_k t - b_k \sin 2\pi f_k t] \\
 &= \frac{1}{2} D(t)
 \end{aligned}
 \tag{12}$$

$$\begin{aligned}
 I'(t) &= \sum_{k=0}^{N-1} [a_k \cos 2\pi (f_c + f_k) t - b_k \sin 2\pi (f_c + f_k) t] \times (-\sin 2\pi f_c t) \\
 &= \frac{1}{2} \sum_{k=0}^{N-1} [a_k \sin 2\pi f_k t + b_k \cos 2\pi f_k t] \\
 &= \frac{1}{2} I(t)
 \end{aligned}
 \tag{13}$$

Note that, in Equations (12) and (13), the term of  $2f_c$  is neglected. Equations (12) and (13) coincide with the real-number and imaginary-number parts of Equation (3) representing a complex baseband signal on the transmission side, respectively. Therefore, as has been described above, an original signal can be extracted by performing an N-point sampling DFT arithmetic operation.

#### (e) Differential Encoding

Although the frequency conversion scheme on reception side has been described in (d), it is very difficult to form a reception local frequency synchronized with a transmission local frequency  $\omega_c$  in the OFDM scheme. When the reception local frequency includes a frequency error (asynchronous state), a demodulated vector is rotated as a result, and demodulation cannot be easily performed by the absolute phase. For this reason, information is not represented by the absolute phase, and the information is represented by the magnitude of phase rotation. This is called differential encoding. According to this scheme, even if there is some frequency error, demodulation can be performed.

#### (e-1) Differential Encoder

FIG. 24 is a view for explaining a differential encoder on transmission side. The logical equation of a differential encoder 21 is given by:  
[Equation 14]

$$d_I(k) = \frac{D_I(k) \cdot d_{I-1}(k)}{1 + j} \quad (14)$$

The differential encoder 21 is to convert data  $D_L(k)$  which is complex-expressed by the following equations:  
[Equation 15]

$$D_I(k) = A_I(k) + jB_I(k) \quad d_I(k) = a_I(k) + jb_I(k)$$

into  $d_L(k)$  by the above logical equation.

A differential code,

in case of (1)  $[A_L(k), B_L(k)] = (1, 1)$ ,

is given by the following equation:

[Equation 16]

$$\begin{aligned} D_I(k) &= A_I(k) + jB_I(k) \\ &= 1 + j \end{aligned}$$

When this value is put into Equation (14), the following equation can be obtained:  
[Equation 17]

$$\begin{aligned} d_I(k) &= \frac{(1 + j) \cdot d_{I-1}(k)}{1 + j} \\ &= d_{I-1}(k) \end{aligned}$$

the phase does not change.

In case of (2)  $[A_L(k), B_L(k)] = (-1, -1)$ ,  
the following equation can be obtained:

[Equation 18]

$$D_I(k) = -1 - j$$

$$d_I(k) = \frac{-(1+j) \cdot d_{I-1}(k)}{1+j}$$

$$= -d_{I-1}(k)$$

5

the phase is inverted, i.e., the phase shifts by  $\pi$ .

In case of (3)  $[A_L(k), B_L(k)] = (1, -1)$ ,

the following equation is established:

10 [Equation 19]

$$D_I(k) = 1 - j$$

15

$$d_I(k) = \frac{(1-j) \cdot d_{I-1}(k)}{1+j}$$

$$= -j \cdot d_{I-1}(k)$$

$$= e^{-j\frac{\pi}{2}} \cdot d_{I-1}(k)$$

20

the phase shifts clockwise by  $\pi/2$ .

In case of (4)  $[A_L(k), B_L(k)] = (-1, 1)$ ,

the following equation is established:

25 [Equation 20]

$$D_I(k) = 1 - j$$

30

$$d_I(k) = \frac{(-1+j) \cdot d_{I-1}(k)}{1+j}$$

$$= j \cdot d_{I-1}(k)$$

$$= e^{j\frac{\pi}{2}} \cdot d_{I-1}(k)$$

35

the phase shifts counterclockwise by  $\pi/2$ .

40

(e-2) Differential Decoder

On the basis of Equation (14), the following equation is obtained:

[Equation 21]

45

$$D_I(k) = (1+j) \frac{d_I(k)}{d_{I-1}(k)} \quad (15)$$

50 A differential decoder 22 is to convert data  $d_L(k)$  into  $D_L(k)$  according to the logical equation represented by Equation (15) as shown in FIG. 25. Therefore, in accordance with the cases (1) to (4) of the differential decoder, the following differential decoding results (1) to (4) are output.

[Equation 22]

55

(1)

In case of



$$\frac{d_I(k)}{d_{I-1}(k)} = 1$$

$$D_I(k) = 1 + j \quad [A_I(k), B_I(k)] = (1, 1)$$

(2)  
In case of

$$\frac{d_I(k)}{d_{I-1}(k)} = -1$$

$$D_I(k) = -1 - j \quad [A_I(k), B_I(k)] = (-1, -1)$$

(3)  
In case of

$$\frac{d_I(k)}{d_{I-1}(k)} = e^{j\frac{\pi}{2}}$$

$$\begin{aligned} D_I(k) &= j(1 + j) \\ &= -1 + j \quad [A_I(k), B_I(k)] = (-1, 1) \end{aligned}$$

(4)  
In case of

$$\frac{d_I(k)}{d_{I-1}(k)} = e^{-j\frac{\pi}{2}}$$

$$\begin{aligned} D_I(k) &= -j(1 + j) \\ &= 1 - j \quad [A_I(k), B_I(k)] = (1, -1) \end{aligned}$$

#### (f) Blocks of Transmission System and Reception System

According to the above description, a transmission system and a reception system in digital audio broadcast using the OFDM scheme have arrangements shown in FIGS. 26A and 26B, respectively. In a frequency converter 14 in the transmission system, reference numeral 14d denotes an oscillator for outputting a cos signal ( $\cos \omega_c t$ ) of a frequency  $f_c$ , and reference numeral 14e denotes a phase shifter for shifting the phase of the cos signal by  $-90^\circ$  to output  $-\sin \omega_c t$ . In a frequency converter 15 in the reception system, reference numeral 15e denotes an oscillator for outputting a cos signal ( $\cos \omega_c t$ ) of the frequency  $f_c$ , and reference numeral 15f is a phase shifter for shifting the phase of the cos signal by  $-90^\circ$  to output  $-\sin \omega_c t$ . A cos wave and a sin wave (carrier) in the transmission system are called transmission local signals, and a cos wave and a sin wave in the reception system are called reception local signals.

On the transmission side, a DAB frame is constituted by a known phase reference symbol and M data symbols. Each symbol is divided into N groups each having two bits, the first and second data of each group are encoded as a real-number part and an imaginary-number part, respectively. The real-number part and imaginary-number part of a differential code are sequentially input to a Fourier transformer 11, the real-number part and the imaginary-number part output from the Fourier transformer are converted into analog signals, and the analog signals are multiplied by the cos and sin waves of the transmission local frequency  $f_c$ , respectively. The multiplication results are synthesized to be radiated in the space.

On the transmission side, the signal radiated in the space is received, and the received signal is multiplied by cos and sin waves of a reception local frequency. The multiplication results are converted into digital signals, and the digital signals are input to a Fourier transformer 18. A real-number part and an imaginary-number part output from the Fourier

transformer are differentially decoded, and the decoded signals are sequentially output as first and second data serving as original data. The Fourier transformer 18 executes a Fourier transformation process on the basis of the generation timing of a DFT window signal. More specifically, a window signal generator (not shown) detects a null signal portion formed between frames to output a DFT window signal serving as a Fourier transformation execution timing of each symbol. The Fourier transformer 18 executes Fourier transformation on the basis of the generation timing of the DFT window signal.

FIG. 27 is a timing chart for explaining a DAB frame and window signals. The start portion of the DAB frame is called a synchronous channel, and is constituted by a null signal portion NULL and a phase reference symbol PRS (Phase Reference Symbol). A guard interval GIT of 62  $\mu$ s (in case of mode 2) is formed before the phase reference symbol portion PRS to reduce the influence of a multipath. A predetermined number (= m) of symbols are arranged after the synchronous channel, and a guard interval of 62  $\mu$ s is formed before each symbol to reduce the influence of a multipath as in the above description. The contents of the second-half portion of a corresponding symbol are repeatedly inserted into the respective guard intervals.

The null signal portion NULL is formed to find the start of a frame. The phase reference symbol PRS is used as a reference signal for differential decoding or is used for an impulse response arithmetic operation of a transmission path. The phase reference symbol PRS receives a unique pattern (known) inherent in each frame. The PRS window is a window arranged at a predetermined time position with reference to the detected null signal portion NULL. The DFT window indicates the timing of a DFT arithmetic operation of each symbol.

When a multipath is generated, as shown in FIGS. 28A to 28D, in addition to a direct wave, a plurality of reflective waves are generated. More specifically, the symbol position of the direct wave is as shown in FIG. 28A, and the symbol positions of the reflective waves 1 to 3 generated by a multipath are as shown in FIGS. 28B to 28D because of delay. As a result, a synthesized wave between the direct wave and the reflective waves becomes the wave shown in FIG. 28E. Reference symbol  $\Delta$  denotes a guard interval. The same contents as those of the second-half portion of the symbol B are repeatedly inserted into the guard interval  $\Delta$ .

In the synthesized wave, zone a indicates a guard interval zone which is interfered from adjacent symbol A due to a multipath; zone b, a guard interval zone which is not interfered from symbol A; and zone c, the zone of symbol B. A DFT window WDW must be set at a position where an interest symbol is DFT-demodulated without being influenced by an adjacent symbol. For example, the DFT window WDW is set at a position shown in FIG. 28E. In this case, when the DFT window is out of the zone of symbol B, the contents of a portion d which is out of the zone can be loaded from a guard interval portion d'. For this reason, the Fourier transformer can correctly DFT-demodulate symbols.

In this manner, even if a reflective wave is generated by a multipath, when delay from the direct wave is set within the guard interval period, an interest symbol is not interfered from an adjacent symbol such that the DFT window position is set as described above. However, when a reflective wave having delay from the direct wave exceeding the guard interval period is generated, the reflective wave interferes with the adjacent symbol. When the interference of the adjacent symbol occurs, the DFT window must be set at a position where the interference is minimized. However, there is no art in which the above measure is arranged. Therefore, the interference causes the degradation of tone quality and serves as a factor that generates multipath noise.

As described above, even if a reflective wave is generated by a multipath, when delay from the direct wave is set within the guard interval period, the symbol is not interfered from an adjacent symbol such that the DFT window position is properly set. However, when the receiver is on a vehicle, a multipath environment changes every moment. For this reason, the DFT window must be set at a position where interference of the DFT window caused by a symbol with respect to the next multipath environment change is made as small as possible. However, there is no art in which the above measure is arranged. Therefore, the interference causes the degradation of tone quality and serves as a factor that generates multipath noise.

## SUMMARY OF THE INVENTION

Therefore, it is the first object of the present invention to set a DFT window at a position where interference from an adjacent symbol is minimum.

It is the second object of the present invention to set a DFT window at a position where the DFT window is not easily interfered by a symbol with respect to the next multipath environment change even if a multipath environment changes every moment.

According to the present invention, the first object is achieved by a receiver in digital audio broadcast, comprising a DFT window generator for generating a DFT window serving as a Fourier transformation execution timing of each symbol to input the DFT window to the Fourier transformer, and an impulse response arithmetic section for arithmetically operating impulse response of a transmission path on the basis of a Fourier transformation output of the phase reference symbol, wherein the DFT window generator sequentially shifts the position of the window having the width  $\Delta$ , calculates the energy of impulse response in the window at respective positions to obtain a window position where the

maximum energy can be obtained, and determines a generation timing of the DFT window on the basis of the window position where the maximum energy can be obtained to input the generation timing to the Fourier transformer.

According to the present invention, the second object is achieved by a receiver in digital audio broadcast, comprising a DFT window generator for generating a DFT window serving as a Fourier transformation execution timing of each symbol to input the DFT window to the Fourier transformer, and an impulse response arithmetic section for arithmetically operating impulse response of a transmission path on the basis of a Fourier transformation output of the phase reference symbol, wherein the DFT window generator sequentially shifts the position of the window having the guard interval width  $\Delta$ , calculates the energy of impulse response in the window at respective positions to obtain a window position  $x$  where the maximum energy can be obtained, when window positions indicating the maximum energy continue, calculates the width of the continuous zone, determines the position of the window such that an extension range of impulse response is located at the window center of the width  $\Delta$  by using the window position  $x$  and the width, and determines a generation timing of the DFT window on the basis of the window position to input the generation timing to the Fourier transformer.

## BRIEF DESCRIPTION OF THE DRAWINGS

FIG. 1 is a model of a transmission path.

FIG. 2 is a view for explaining impulse response.

FIG. 3 is a view for explaining a signal in a phase reference symbol.

FIG. 4 is a graph showing impulse response.

FIG. 5 is a graph for explaining impulse response depending on the presence/absence of delay.

FIG. 6 is a view for explaining the relationship between impulse response and a guard interval in a state wherein a multipath is generated.

FIG. 7 is a view for explaining the first principle of the present invention.

FIG. 8 is a view for explaining the second principle of the present invention (part 1).

FIG. 9 is a view for explaining the second principle of the present invention (part 2).

FIG. 10 is a view showing the arrangement of a DAB receiver according to the present invention.

FIG. 11 is a flow chart showing a process of determining a DFT window position.

FIG. 12 is a flow chart showing another process of determining a DFT window position.

FIG. 13 is a view showing the theoretical arrangement of a transmitter in digital audio broadcast.

FIG. 14 is a view for explaining the function of a frequency multiplexer.

FIG. 15 is a view for explaining a symbol.

FIG. 16 is a view showing the theoretical arrangement of a receiver in digital audio broadcast.

FIG. 17 is a view for explaining  $D(m)$ .

FIG. 18 is the characteristics of an ideal filter.

FIG. 19 is a view showing the arrangement of a main part of a transmitter using IDFT.

FIG. 20 is a view for explaining a sampling theorem.

FIG. 21 is the arrangement of a main part of a receiver using DFT.

FIG. 22 is the arrangement of an orthogonal balance modulation scheme.

FIG. 23 is the arrangement of an orthogonal frequency conversion scheme.

FIG. 24 is a view for explaining a differential encoder.

FIG. 25 is a view for explaining a differential decoder.

FIG. 26 is the arrangements of a transmission system and a reception system.

FIG. 27 is a view for explaining a DAB frame.

FIG. 28 is a view for explaining FFT window position control in a multipath environment.

## DESCRIPTION OF THE PREFERRED EMBODIMENTS

### (a) Impulse Response of Transmission Path

FIG. 1 is a model of a transmission path. Reference numeral 51 denotes a DAB transmitter; 52, a DAB receiver; and 53, a transmission path. Reference symbol  $x(n)$  denotes a transmission signal;  $h(n)$ , the characteristic of the transmission path; and  $y(n)$ , a reception signal. The respective signals have the following relationship:

$$X(k) \cdot H(k) = Y(k)$$

i.e.,

$$H(k) = Y(k)/X(k) \quad (16)$$

where  $X(k)$ ,  $H(k)$ , and  $Y(k)$  are obtained by performing Fourier transformation to  $x(n)$ ,  $h(n)$ , and  $y(n)$ , respectively.

Due to the above relationship, when  $x(n)$  and  $y(n)$  or  $X(k)$  and  $Y(k)$  are known,  $h(n)$  (impulse response) is derived, and a multipath environment can be estimated by the impulse response. FIG. 2A shows impulse response obtained when no multipath is generated, and FIG. 2B shows impulse response obtained when a multipath is generated. More specifically, a reference phase symbol (PRS) included in the start of the frame shown in FIG. 27 is represented by  $X(k)$ , and the received PRS is represented by  $Y(k)$ , thereby deriving  $h(n)$ .

In DAB, as  $X(k)$ , a signal expressed by the following equation is used:

$$X(k) = e^{j\pi k^2/4} \quad (-m \leq k \leq -1, 1 \leq k \leq m) \quad 0 \text{ (} m \text{ does not satisfy the above conditions)}$$

This signal is illustrated in FIG. 3 (carrier exists in the range represented by  $-m \leq k \leq -1$  and  $1 \leq k \leq m$ ). Therefore, the transmission path has no delay time,  $H(k)$  is given by the following equation:

$$H(k) = Y(k)/X(k) = 1 \quad (-m \leq k \leq -1, 1 \leq k \leq m) \quad 0 \text{ (} m \text{ does not satisfy the above conditions)}$$

In the above equation, assume that  $H(1) = 1$  is approximately established. In this case, it is apparent that inverse DFT of  $H(k)$  is given by the following sinc function.

$$h(n) = (m/N) \cdot [\sin(n\pi m/N)/(n\pi m/N)] \quad (17)$$

More specifically, since  $m = 1536$  and  $N = 2048$  are satisfied in mode I of the DAB, the  $h(n)$  is given by  $h(0) = 1$  where  $n = 0$ , and the  $h(n)$  satisfies  $h(n) \ll 1$  where  $n \neq 0$ . As shown in FIG. 4, a sharp peak appears at a position where  $h(n)$  is maximum, i.e.,  $n = 0$ . Therefore, when the transmission path has no delay time, an impulse response shown in FIG. 5A is obtained. However, when the transmission path has a delay time corresponding to  $n_0$  sampling, the impulse response is expressed by  $h(n - n_0)$ . For this reason, when  $n$  is substituted for  $n - n_0$  in Equation (17), the impulse response changes into that shown in FIG. 5B, and an impulse appears at a position which shifts by  $n_0$ . More specifically, when a delayed reflective wave is generated by a multipath, a plurality of impulses are generated as shown in FIG. 2B.

#### (b) Principle of First Invention

When a reflective wave is generated by a multipath, and the impulse response of the transmission path has an extension equal to or larger than the width  $\Delta$  of the guard interval, a window is interfered from an adjacent symbol. In the case shown in FIG. 6A, impulses IPL6 to IPL8 which exceed the range of the width  $\Delta$  of the guard interval become interference signals. More specifically, when the DFT window 51 is set at the position shown in FIG. 6A, the impulses IPL6 to IPL8 serve as interference signals, and the other impulses serve as signals which contribute to the DFT process of an interest symbol.

Similarly, when the DFT window 51 is set at the position shown in FIG. 6B, the impulses IPL1 and IPL7 to IPL8 serve as interference signals, and the other impulses IPL2 to IPL6 serve as signals which contribute to the DFT process of the interest symbol.

When the DFT window is set at a position where the energy of the interference signals is minimum and the energy of the other signals is maximum, adjacent symbol interference from a multipath can be minimized.

For this reason, as shown in FIG. 7, the window 52 having a width equal to the width  $\Delta$  of the guard interval is assumed. The position of the window 52 is sequentially shifted, and energy (total sum of amplitudes of impulses) of impulses set in the width  $\Delta$  of the window 52 is calculated at respective positions to obtain a position where the energy is maximum. When the DFT window 51 is set at the position where the energy is maximum, the influence of interference can be minimized.

#### (c) Principle of Second Invention

Even if a reflective wave is generated, as shown in FIG. 8, an extension  $\tau$  of impulse response of the transmission path is smaller than the width  $\Delta$  of the guard interval. In this case, the position of the DFT window is set such that the impulse is within the start width  $\Delta$  of the DFT window 51, the DFT window is not interfered from the adjacent symbol. However, when the receiver is on a vehicle, a multipath environment changes every moment. For this reason, the DFT window must be set at a position where interference of the DFT window caused by a symbol with respect to a multipath environment change is made as small as possible. For this purpose, the extension range  $\tau$  of the impulse is preferably set at a central position in the start width  $\Delta$  of the DFT window 51.

Assume a window 52 having a width equal to the guard interval width  $\Delta$ , and the position of the window 52 is sequentially shifted, and the energy (total sum of amplitudes of impulses) of impulses set in the width  $\Delta$  of the window 52 is calculated at respective positions to obtain a position  $x_0$  (position indicated by (2) in FIG. 8) where the energy is maximum. When the DFT window 51 is set at the position where the energy is maximum, the influence of interference can be minimized. When window positions each indicating a maximum energy  $P_{\max}$  continue (zone between (2) and (3)), and the width  $(\Delta - \tau)$  of the continuous zone is calculated. Thereafter, the position (see the dotted line in FIG. 8) of the window 52 is set such that the extension range of impulses is located at the center of the window 52 by using the window position  $x_0$  and the width  $(\Delta - \tau)$ . More specifically, as shown in FIG. 9, the position being apart from the position  $x_0$  at a distance of  $(\Delta - \tau)/2$  is set as the start edge position of the window 52, and the DFT window 51 is set at the same position as the start edge position. In this manner, margins for the advance/delay of the impulse can be set to be  $(\Delta - \tau)/2$ , and the DFT window 51 can sufficiently cope with the next multipath environment change. Therefore, symbol interference with the DFT window 51 can be suppressed.

#### (d) Embodiment of the Present Invention

##### (d-1) Arrangement of DAB Receiver

FIG. 10 is a view showing the arrangement of a DAB receiver according to the present invention.

Reference numeral 60 denotes a reception antenna; 61, an RF signal demodulator for DAB which multiplies a received signal by cos and sin waves of a carrier frequency to output baseband analog signals  $D(t)$  and  $I(t)$ ; 62, an AD converter for converting the baseband analog signals  $D(t)$  and  $I(t)$  into digital data  $D(m)$  and  $I(m)$  at a predetermined sampling frequency; 63, a sampling pulse generator for outputting a sampling pulse; 64, a null signal detector for detecting a null signal portion between DAB frames to output a null detection signal NDL; and 65, a DFT window generator for outputting DFT window signals (including a PRS window signal) serving as Fourier transformation execution timings of symbols constituting a DAB frame. The DFT window generator 65 determines a DFT window position according to the process (to be described later) to output a DFT window signal.

Reference numeral 66 denotes a Fourier transformation/differential decoder for performing a Fourier transformation process to the digital data  $D(m)$  and  $I(m)$  in the PRS window and the DFT window and differentially decoding the digital data  $D(m)$  and  $I(m)$  to demodulate  $X(k)$  (see Equation (16)) and audio code data (e.g., MPEG audio data); 67, an audio signal decoder for decoding the MPEG audio data into a PCM audio data; 68, a DA converter for converting the PCM audio data into analog data; 69, an amplifier; 70, a loudspeaker; 71, an operation key unit; 72, a display unit; and 73, a controller for performing tuning control or other control. Reference numeral 74 denotes an impulse response arithmetic section for arithmetically operating an impulse response by using the Fourier transformation output  $X(k)$  in the PRS window period on the basis of Equation (16).

##### (d-2) Process of Determining DFT Window Position

FIG. 11 is a flow chart showing a process of determining a DFT window position.

When the DFT window generator 65 receives an impulse response result from the impulse response arithmetic section 74, the start edge of the window 52 (see FIG. 7) having a guard interval width  $\Delta$  is set at a position slightly before the position of impulse IPL1 (step 101). At this position, the total sum (energy of impulse response)  $P$  of amplitudes of all impulses set in the width of the window 52 is calculated (step 102) to check whether the energy  $P$  is the maximum energy  $P_{\max}$  (initial value of  $P_{\max}$  is 0) or more (step 103). If  $P > P_{\max}$  is established,  $P \rightarrow P_{\max}$  is set, the start edge position  $x$  of the window 52 is stored as a DFT window position (step 104), and the position of the window 52 is shifted to the right by one step (step 105). On the other hand, if  $P \leq P_{\max}$  is established in step 103, the position of the window 52 is shifted to the right by one step without updating  $P_{\max}$  (step 105).

It is checked whether a shift amount becomes a set value (e.g.,  $\Delta$ ) (step 106). If NO in step 106, the steps following step 102 are repeated to search for the window position having the maximum energy.

When the window position  $x$  having the maximum energy is obtained as described above, the DFT window position is determined such that the start edge of the DFT window is located at the window position  $x$ , and a DFT window signal is generated (step 107).

##### (d-3) Entire Operation

The RF signal demodulator 61 for DAB multiplies a received signal by cos and sin waves of the carrier frequency to output baseband analog signals  $D(t)$  and  $I(t)$ , and the AD converter 62 converts baseband analog signals  $D(t)$  and  $I(t)$  into digital data  $D(m)$  and  $I(m)$  on the basis of a sampling pulse output from the sampling pulse generator 63 to input the digital data  $D(m)$  and  $I(m)$  to the null signal detector 64 and the Fourier transformation/differential decoder 66. While

the above operation is performed, the DFT window generator 65 inputs a DFT window signal and a PRS window signal to the Fourier transformation/differential decoder 66 and the impulse response arithmetic section 74 at a timing calculated in the previous frame according to the process in FIG. 11.

When the Fourier transformation/differential decoder 66 performs a Fourier transformation process to the digital data  $D(m)$  and  $I(m)$  in the PRS window and the DFT window for each symbol, and then differentially decodes the digital data  $D(m)$  and  $I(m)$  to demodulate  $X(k)$  and audio code data (MPEG audio data) and to output them.

The audio signal decoder 67 decodes the MPEG audio data into PCM audio data, and the DA converter 68 converts the PCM audio data into analog data and inputs the analog data to the loudspeaker 70 through the amplifier 69, thereby outputting DAB voice. The impulse response arithmetic section 74 arithmetically operates an impulse response by using the Fourier transformation output in the PRS window period on the basis of Equation (16) and inputs the arithmetic result to the DFT window generator 65.

The null signal detector 64 detects a null signal portion between DAB frames to output a null detection signal NDT. After the DFT window generator 65 receives the null detection signal NDT, when the DFT window generator 65 receives an impulse response from the impulse response arithmetic section 81, the DFT window generator 65 determines a DFT window position in the next frame according to the process in FIG. 11.

Subsequently, when the above operation is repeated, interference can be minimized even in a multipath generation environment, and preferable audio voice can be output from the loudspeaker.

#### (d-4) Modification

As a method of determining the position of the window 52 having the width  $\Delta$ , not only the above method, but also the following method can be used. More specifically, while the position of the window 52 largely shifts step  $a$  ( $1 < a < \Delta$ ) by step  $a$ , the energies in the window at positions are calculated and compared with each other. In this manner, when the position having the maximum energy can be obtained, while the position shifts step by step, energy amounts in the ranges each having the width  $a$  and set before and after the position are calculated and compared with each other to calculate the position having the maximum energy. This position is determined as the DFT window position.

The maximum impulse is detected, and, while the window shifts step by step in the ranges each having the width  $\Delta$  and set before and after the maximum impulse, energy amounts in the window are calculated and compared with each other. In this manner, the DFT window position can also be determined.

#### (e) Another Process of Determining DFT Window Position

FIG. 12 is a flow chart showing another process of determining a DFT window position.

The impulse response arithmetic section 74 arithmetically operates an impulse response by using the Fourier transformation output  $X(k)$  in the PRS window period on the basis of Equation (16), and inputs the arithmetic result to the DFT window generator 65 (step 201). When the DFT window generator 65 receives an impulse response from the impulse response arithmetic section 74, the DFT window generator 65 sets the start edge of the window 52 (see FIG. 8) having the guard interval width  $\Delta$  to a position  $(\Delta + \alpha)$  before the start impulse IPL1. At this position, a total sum (energy of the impulse response)  $P$  of the amplitudes of all impulses set in the width of the window 52 (step 202) to check whether the energy  $P$  is the maximum energy  $P_{\max}$  (initial value of  $P_{\max}$  is 0) or more (step 203). If  $P > P_{\max}$  is established,  $P \rightarrow P_{\max}$  is set, the start edge position  $x$  of the window 52 is stored (step 204), and  $i$  is set to be 0 (step 205).

If  $P > P_{\max}$  is not established in step 203, it is checked whether  $P = P_{\max}$  (step 206). If  $P = P_{\max}$  is established,  $i$  is incremented (step 207), and the position of the window 52 having the width  $\Delta$  is shifted to the right by one step (step 208). In step 206, if  $P \neq P_{\max}$ , the position of the window 52 is shifted to the right by one step without incrementing  $i$  (step 208).

Thereafter, it is checked whether the shift amount becomes a set value (e.g.,  $2\Delta + \beta$ ) (step 209). If the shift amount becomes the set value, the steps following step 202 are repeated. In this manner, the window positions which indicate the maximum energy  $P_{\max}$  continue (zone between (2) and (3) in FIG. 8), and reference numeral  $i$  indicates the width  $(\Delta - \tau)$  of the continuous zone.

If the shift amount becomes the set value, it is checked whether  $i = 0$  is established (step 210). If  $i > 0$  is established,  $i/2$  is calculated (step 211), and a DFT window signal is generated by using the position represented by  $x + i/2$  as the start edge position of the DFT window (step 212). On the other hand, since  $i = 0$  in step 210 means that the extension of the impulse response is the guard interval width  $\Delta$  or more, the DFT window position is determined such that the start edge of the DFT window is located at the position  $x$  indicating the maximum energy, and a DFT window signal is generated (step 213).

With the above arrangement, when the extension of the impulse response is the guard interval width  $\Delta$  or less, margins for the advance/delay of the impulse can be set to be  $(\Delta - \tau)/2$ , and the DFT window 51 can sufficiently cope with

the next multipath environment change. Therefore, symbol interference with the DFT window 51 can be suppressed. In addition, when the extension of the impulse response is the guard interval width  $\Delta$  or more, interference from an adjacent symbol can be minimized.

Although the present invention has been described above with reference to the embodiment, the various changes of the present invention can be effected according to the spirit and scope of the invention described in the claims. The present invention does not exclude these changes.

According to the present invention, the DFT window generator has the following arrangement. That is, the DFT window generator sequentially shifts the position of the window having the width  $\Delta$  and calculates the energy of impulse response in the window at respective positions to obtain a window position where the maximum energy can be obtained, and the DFT window generator determines a generation timing of the DFT window on the basis of the window position where the maximum energy can be obtained to input the generation timing to the Fourier transformer. Therefore, the DFT window can be set at a position where interference from an adjacent symbol is minimum, and preferable DAB voice can be output even in a multipath generation environment.

Further, according to the present invention, the DFT window generator has the following arrangement. That is, the DFT window sequentially shifts the position of the window having the width  $\Delta$  and calculates the energy of impulse response in the window at respective positions to obtain a window position  $x$  where the maximum energy can be obtained. When the window positions each indicating the maximum energy continue, the width  $(\Delta - \tau)$  of the continuous zone is calculated. The position of the window is determined by using the window position  $x$  and the width  $(\Delta - \tau)$  such that the extension range of the impulse response is set at the center of the window having the width  $\Delta$ , and a generation timing of the DFT window is determined on the basis of the window position to input the generation timing to the Fourier transformer. Therefore, even if a multipath environment changes every moment, the DFT window can be set at a position where the DFT window is not easily interfered by a symbol with respect to the next multipath environment change, and preferable DAB voice can be output even in a multipath generation environment.

## Claims

1. A digital audio broadcast receiver in which a frame is constituted by inserting guard intervals each having a width  $\Delta$  before a phase reference symbol and each data symbol,  $2N$  digital data constituting the symbols are divided into  $N$  groups each having two bits, the first data of each group and the second data of each group are sequentially input to an inverse Fourier transformer as a real-number part and an imaginary-number part, respectively, the real-number part and imaginary-number part output from said inverse Fourier transformer are converted into analog signals, the analog signals are multiplied by a cos wave and a sin wave of a carrier frequency  $f_c$ , the multiplication results are synthesized to be radiated in a space, signals radiated in the space are received, the received signals are multiplied by the cos wave and the sin wave of the carrier frequency, the multiplication results are converted into digital signals at a predetermined sampling frequency by an AD converter (62), the digital signals are input to a Fourier transformer (66), and a real-number part and an imaginary-number part output from said Fourier transformer (66) are output as the first and second data, characterized by comprising:

a DFT window generator (65) for generating a DFT window serving as a Fourier transformation execution timing of each symbol to input the DFT window to said Fourier transformer (66); and  
an impulse response arithmetic section (74) for arithmetically operating impulse response of a transmission path on the basis of a Fourier transformation output of the phase reference symbol;

wherein said DFT window generator (65) sequentially shifts the position of the window having the width  $\Delta$ , calculates the energy of impulse response in the window at respective positions to obtain a window position where the maximum energy can be obtained, and determines a generation timing of the DFT window on the basis of the window position where the maximum energy can be obtained to input the generation timing to said Fourier transformer (66).

2. A digital audio broadcast receiver according to claim 1, characterized in that when said DFT window generator (65) receives an impulse response result, said DFT window generator (65) sets the start edge of the window having the guard interval width to a position slightly before the position of a start impulse, and, at this position, calculates energy of impulse response set in the width of the window.
3. A digital audio broadcast receiver according to claim 1, or 2, characterized in that the impulse response is the total sum of amplitudes of all impulses set in the width of the window.
4. A digital audio broadcast receiver according to any of claims 1 to 3, characterized in that

said DFT window generator (65) checks whether the energy of the impulse response set in the width of the window is not less than the maximum energy, if the energy is not less than the maximum energy, sets the energy as the maximum energy, and stores the start edge position of the window as a DFT window position to shift the position of the window in a predetermined direction, and

said DFT window generator (65), if the energy of the impulse response set in the width of the window is not more than the maximum energy, shifts the position of the window in a predetermined direction without updating the energy.

5. A digital audio broadcast receiver according to any of claims 1 to 4, characterized in that the phase reference symbol indicates a PRS window period.

6. A digital audio broadcast receiver in which a frame is constituted by inserting guard intervals each having a width  $\Delta$  before a phase reference symbol and each data symbol,  $2N$  digital data constituting the symbols are divided into  $N$  groups each having two bits, the first data of each group and the second data of each group are sequentially input to an inverse Fourier transformer as a real-number part and an imaginary-number part, respectively, the real-number part and imaginary-number part output from said inverse Fourier transformer are converted into analog signals, the analog signals are multiplied by a cos wave and a sin wave of a carrier frequency  $f_c$ , the multiplication results are synthesized to be radiated in a space, signals radiated in the space are received, the received signals are multiplied by the cos wave and the sin wave of the carrier frequency, the multiplication results are converted into digital signals at a predetermined sampling frequency by an AD converter (62), the digital signals are input to a Fourier transformer (66), and a real-number part and an imaginary-number part output from said Fourier transformer (66) are output as the first and second data,

characterized by comprising:

a DFT window generator (65) for generating a DFT window serving as a Fourier transformation execution timing of each symbol to input the DFT window to said Fourier transformer (66); and  
an impulse response arithmetic section (74) for arithmetically operating impulse response of a transmission path on the basis of a Fourier transformation output of the phase reference symbol;

wherein said DFT window generator (65) sequentially shifts the position of the window having the width  $\Delta$ , calculates the energy of impulse response in the window at respective positions to obtain a window position  $x$  where the maximum energy can be obtained, when window positions indicating the maximum energy continue, calculates the width of the continuous zone, determines the position of the window such that an extension range of impulse response is located at the window center of the width  $\Delta$  by using the window position  $x$  and the width, and determines a generation timing of the DFT window on the basis of the window position to input the generation timing to said Fourier transformer (66).

7. A digital audio broadcast receiver according to claim 6, characterized in that when said DFT window generator (65) receives an impulse response result, said DFT window generator (65) sets the start edge of the window having the guard interval width to a position slightly before the position of a start impulse, and, at this position, calculates energy of impulse response set in the width of the window.

8. A digital audio broadcast receiver according to claim 6 or 7, characterized in that the impulse response is the total sum of amplitudes of all impulses set in the width of the window.

9. A digital audio broadcast receiver according to claim 6, 7 or 8, characterized in that said DFT window generator (65) sequentially shifts the position of the window having the width  $\Delta$  and checks whether the energy of the impulse response set in the width of the window is not less than the maximum energy, if the energy is not less than the maximum energy, sets the energy as the maximum energy, and repeats a process of storing the start edge position  $x$  of the window until a predetermined shift amount is obtained.

10. A digital audio broadcast receiver according to any of claims 6 to 9, characterized in that the phase reference symbol indicates a PRS window period.



FIG. 1

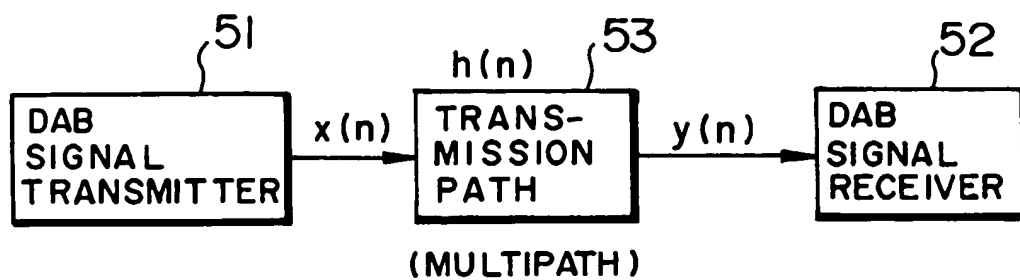


FIG. 2A

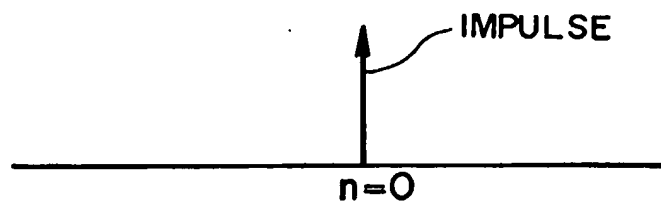


FIG. 2B

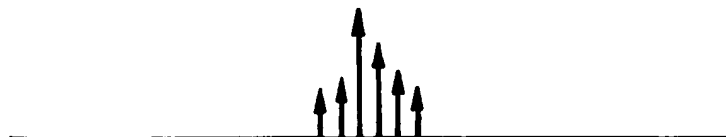


FIG. 3

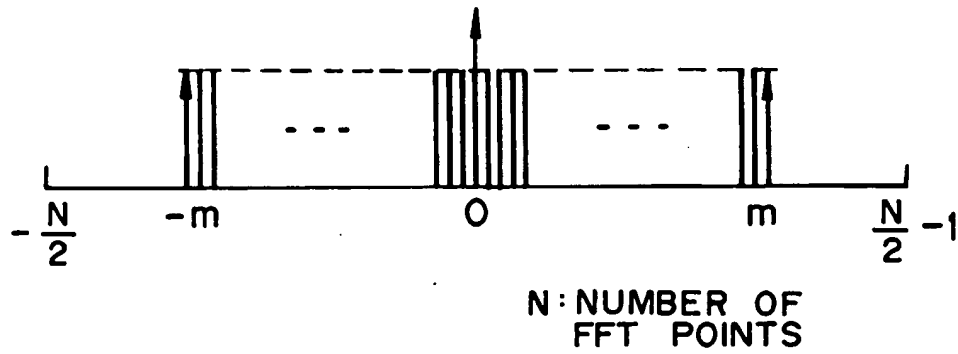


FIG. 4

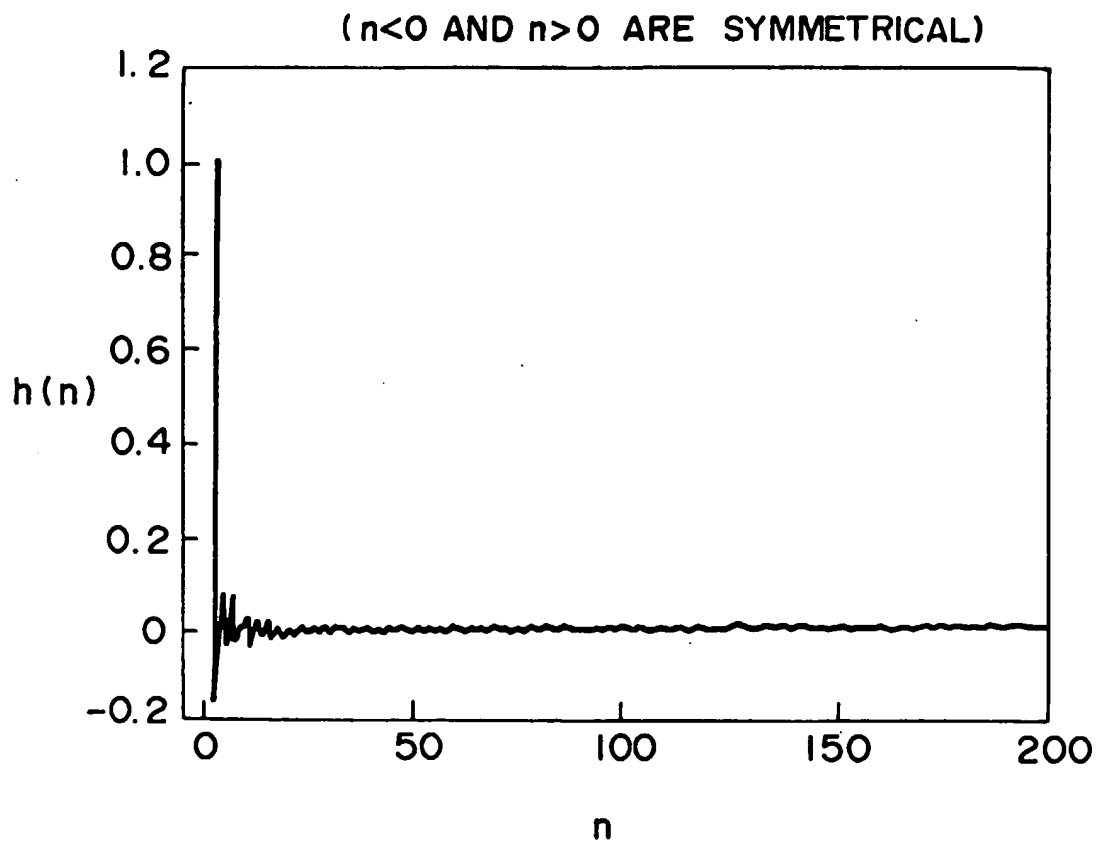


FIG. 5A

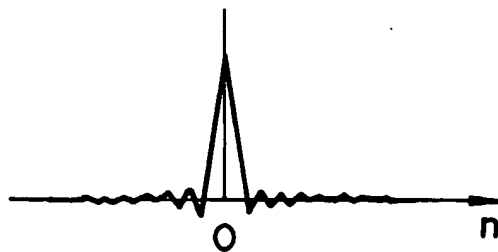


FIG. 5B



FIG. 6

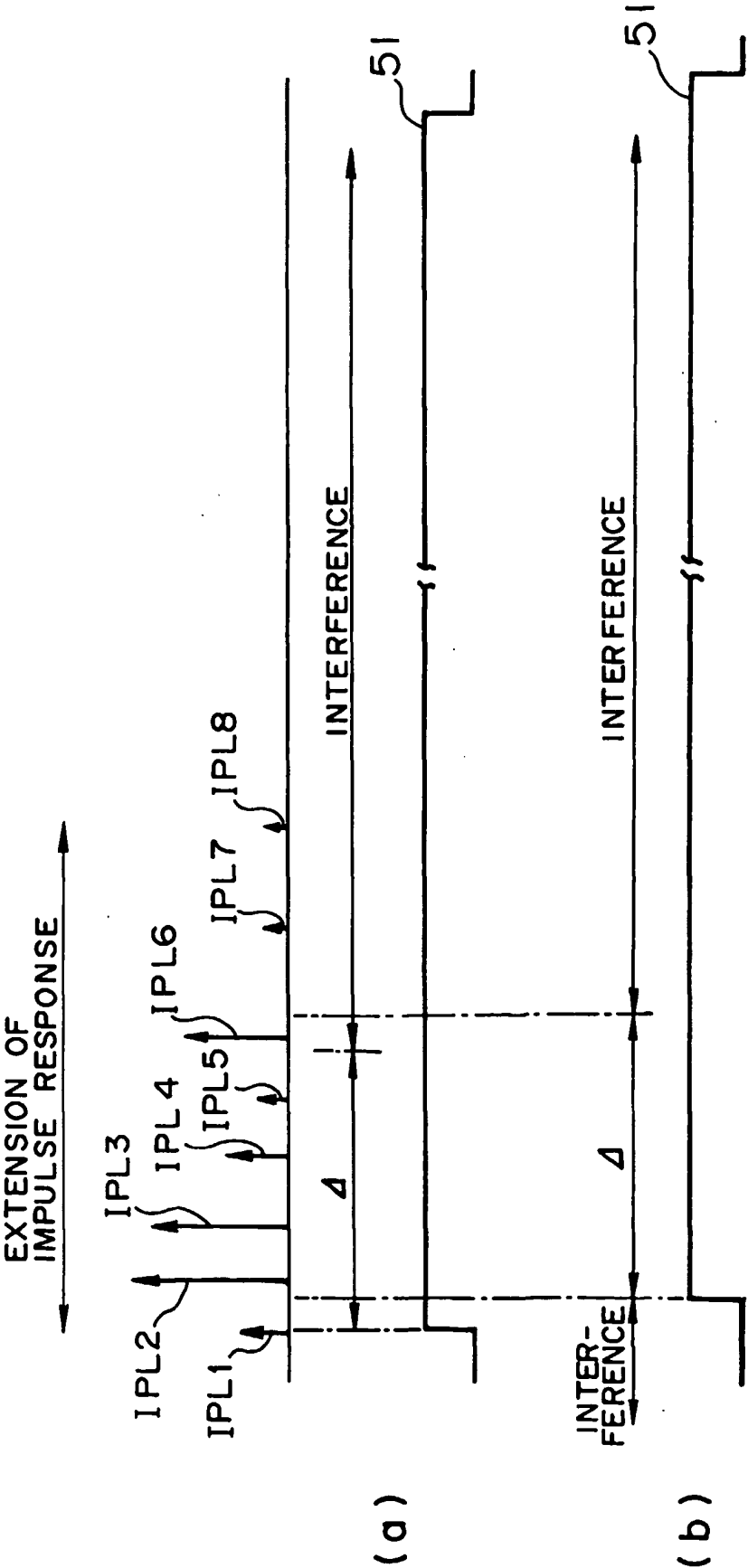


FIG. 7

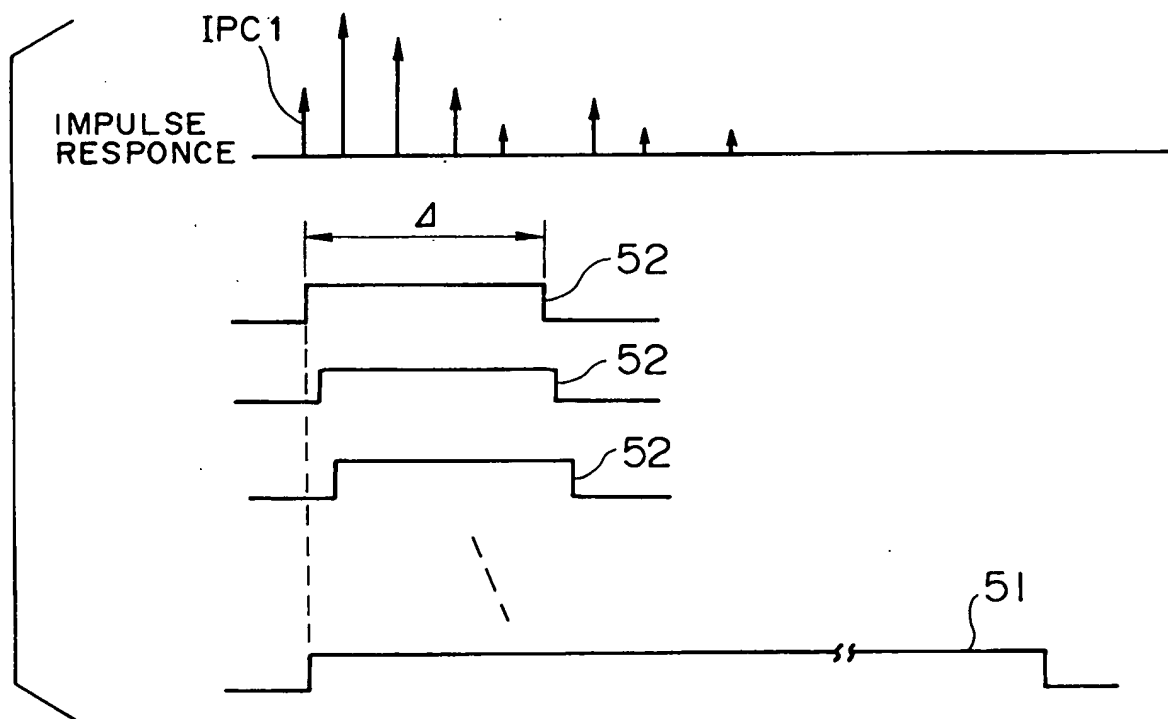


FIG. 8A

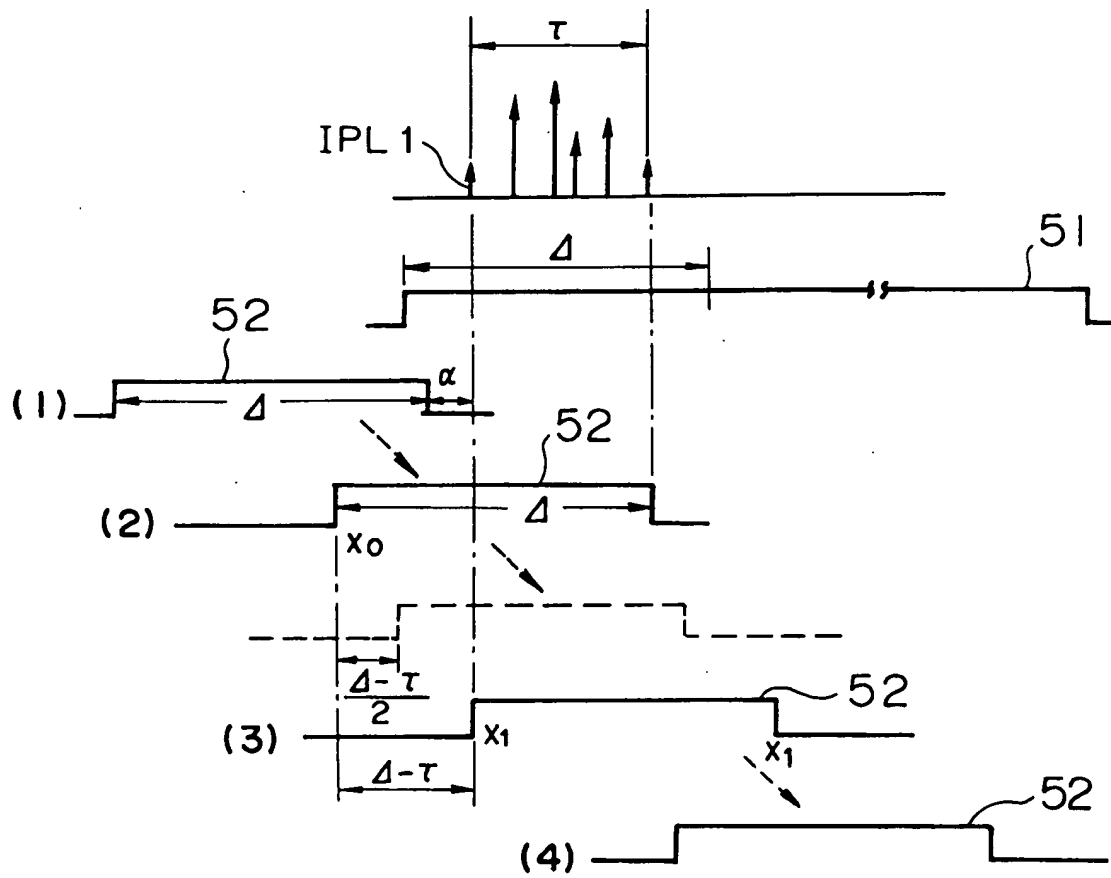


FIG. 8B

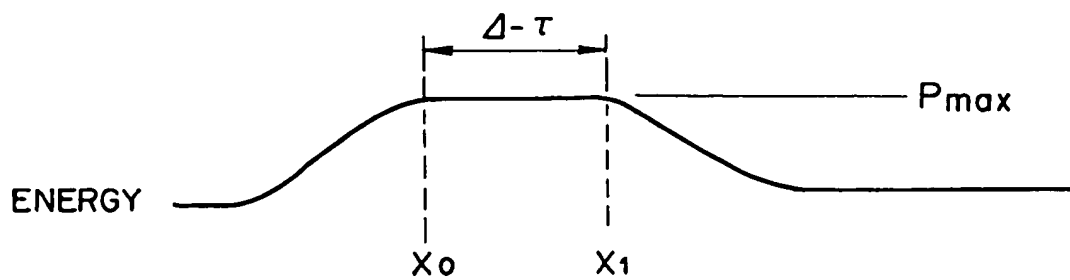


FIG. 9

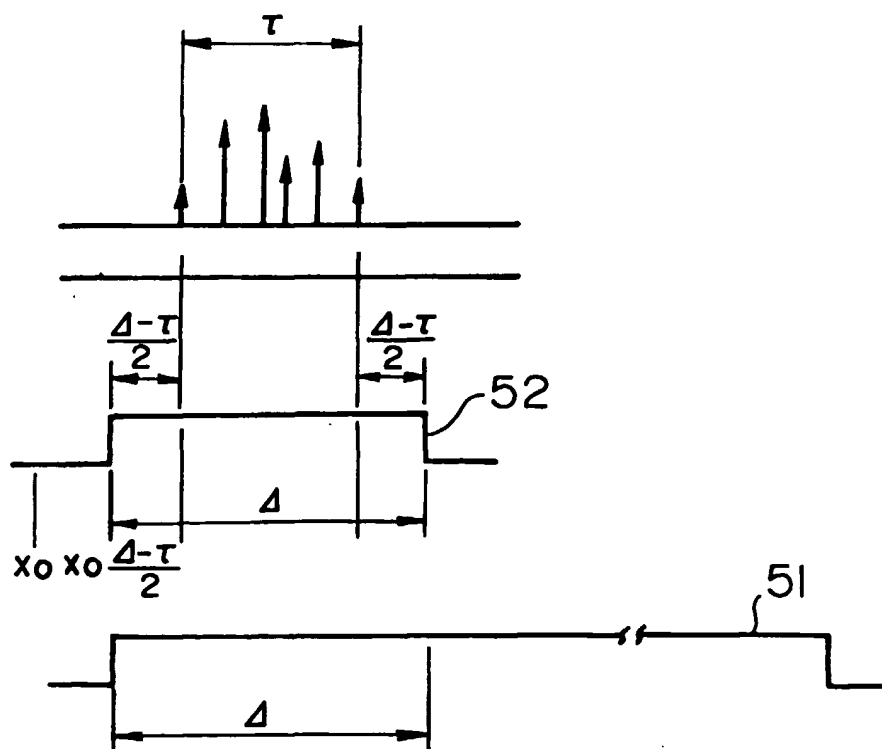


FIG. 10

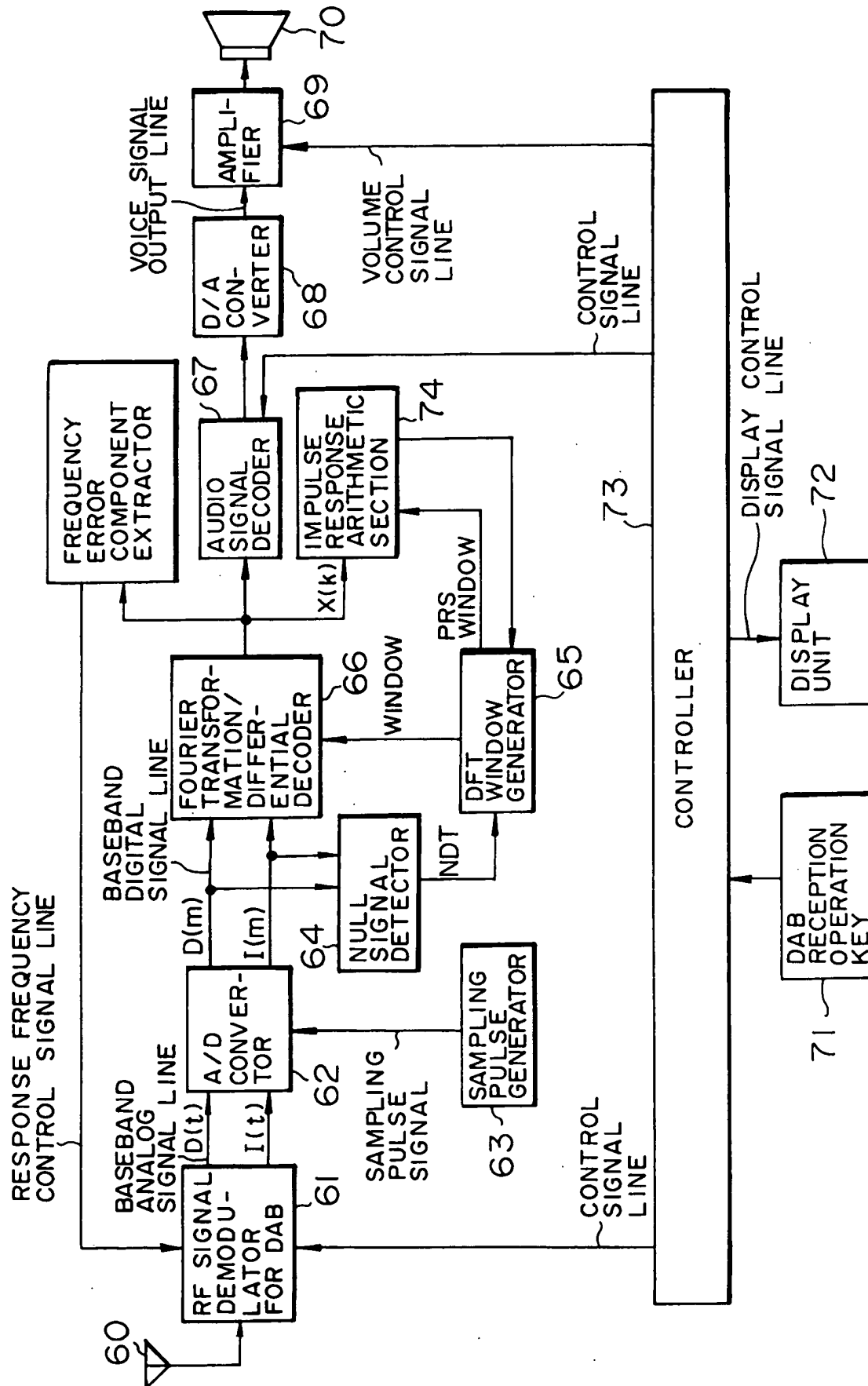




FIG. 11

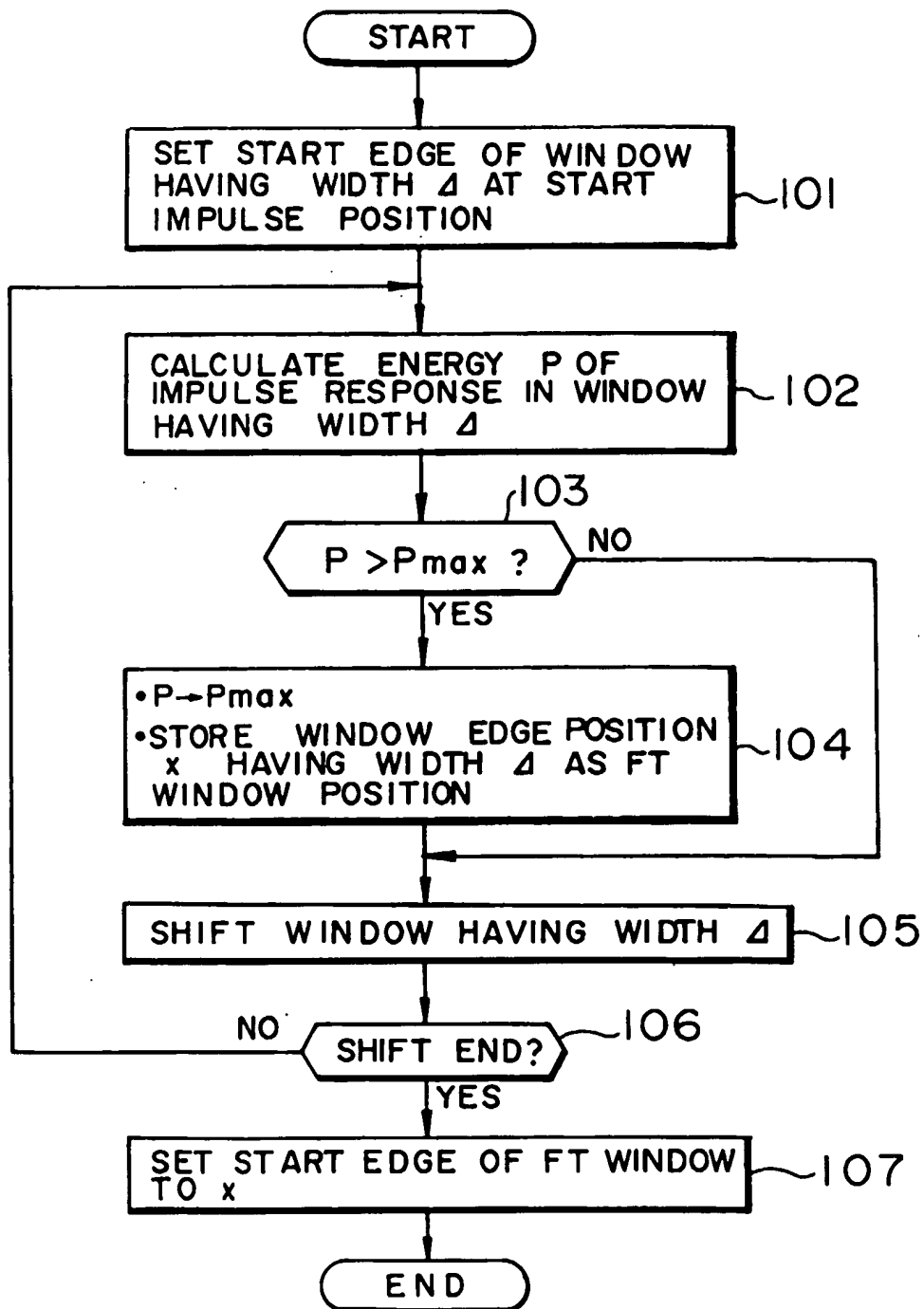


FIG. 12

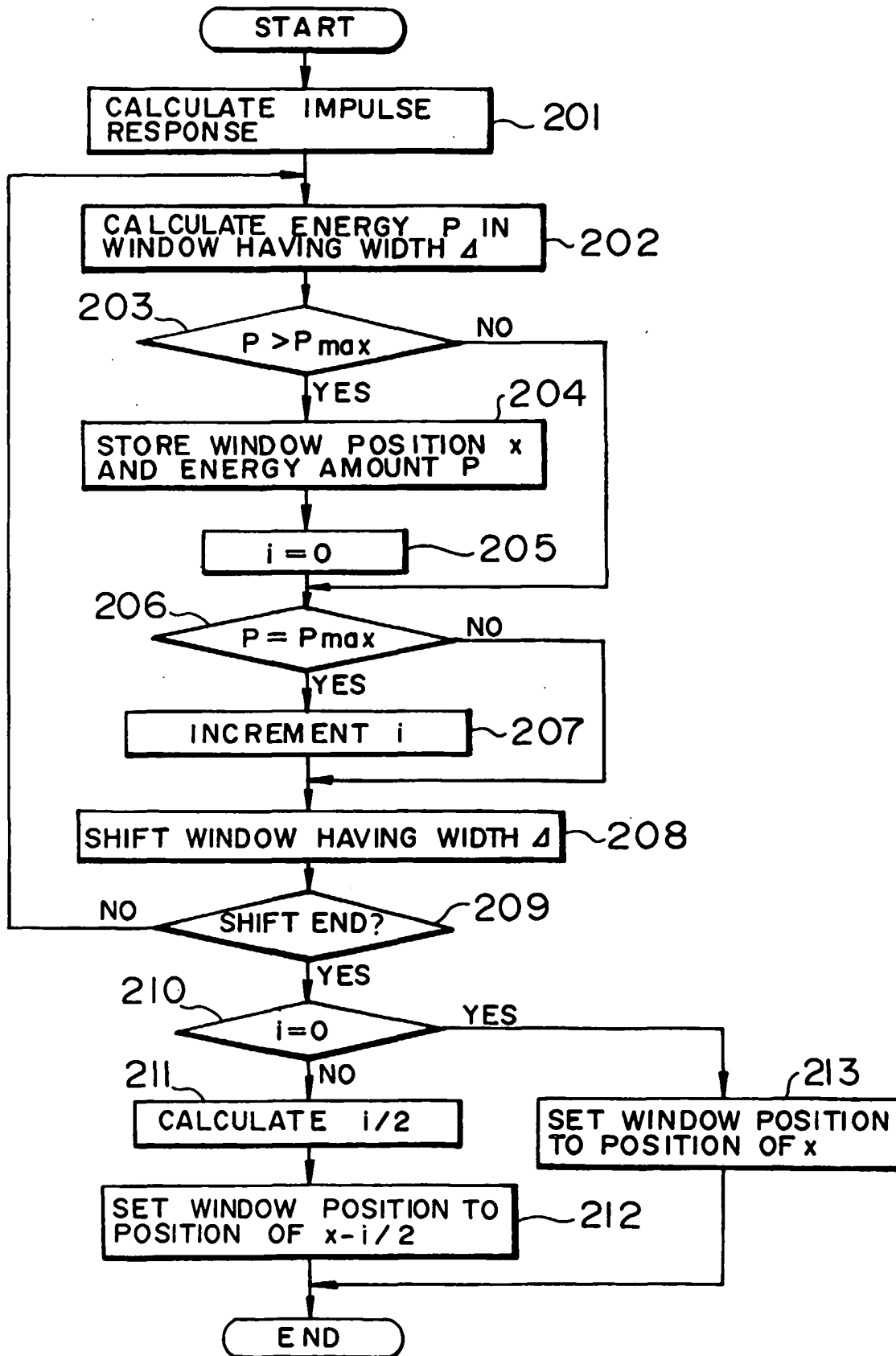
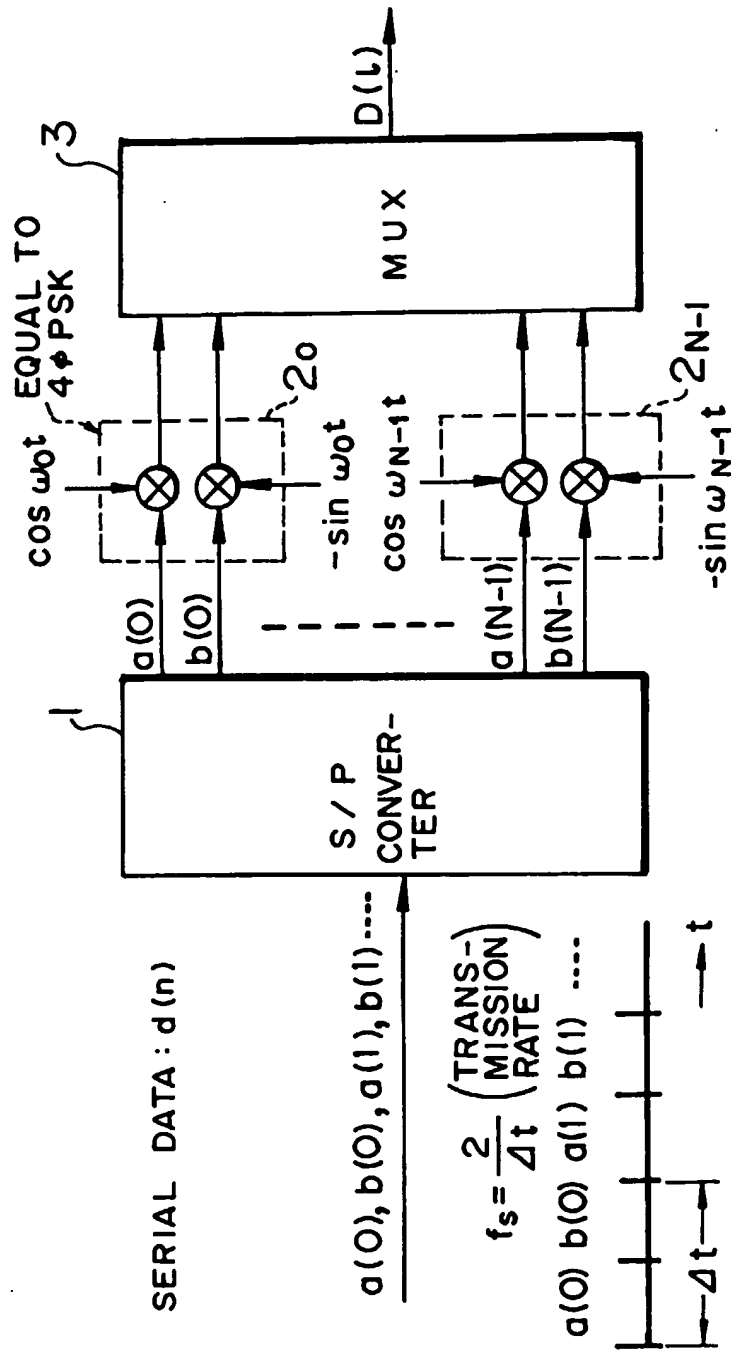


FIG. 13



$$D(t) = \sum_{n=0}^{N-1} \{a(n)\cos \omega_n t + b(n)\sin \omega_n t\}$$

$$\begin{cases} \omega_n = 2\pi f_n \\ f_n = f_0 + n \Delta f \\ \Delta f = \frac{1}{N\Delta t} \end{cases}$$

FIG. 14

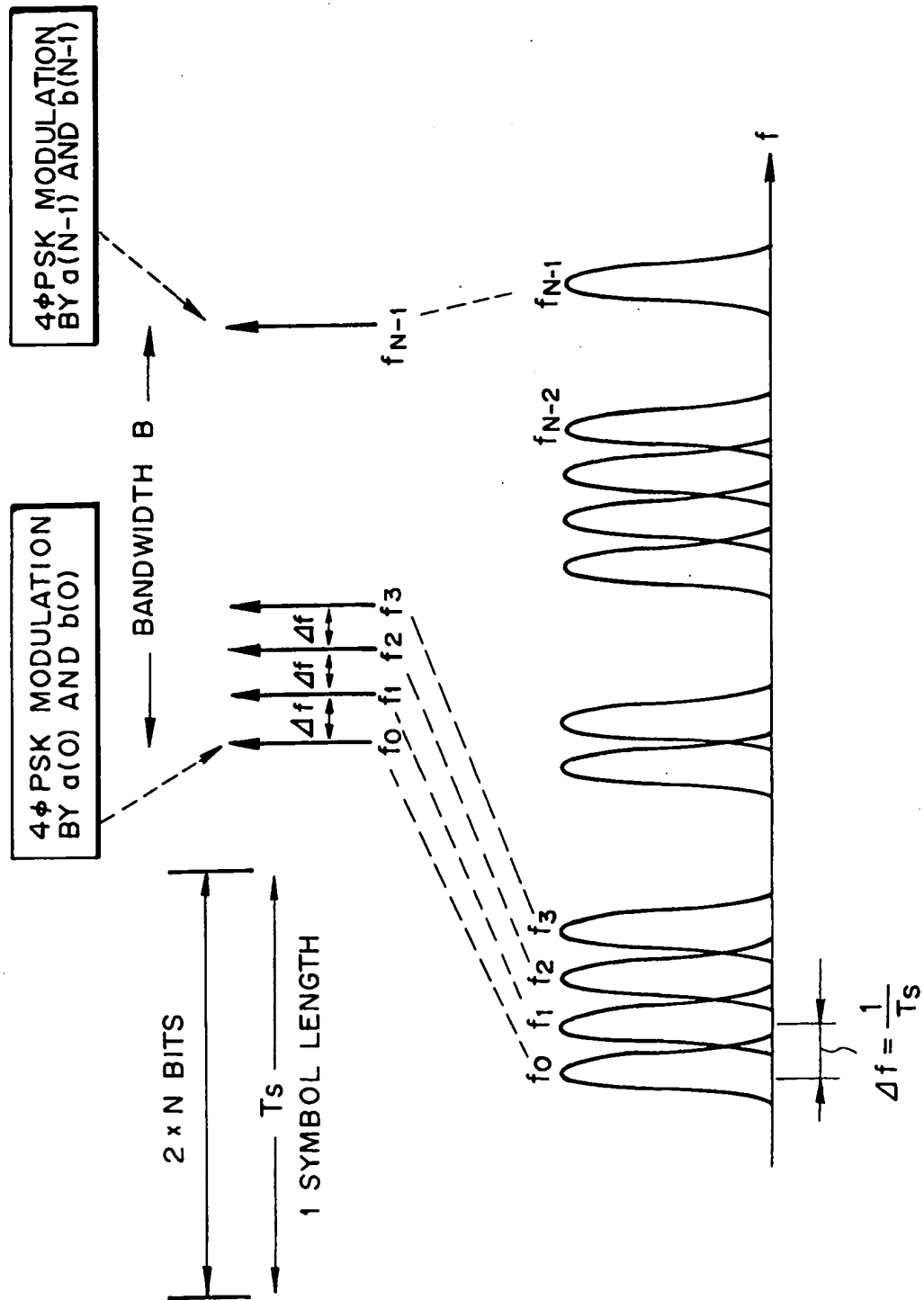


FIG. 15

$$f_s = \frac{2}{\Delta t}$$

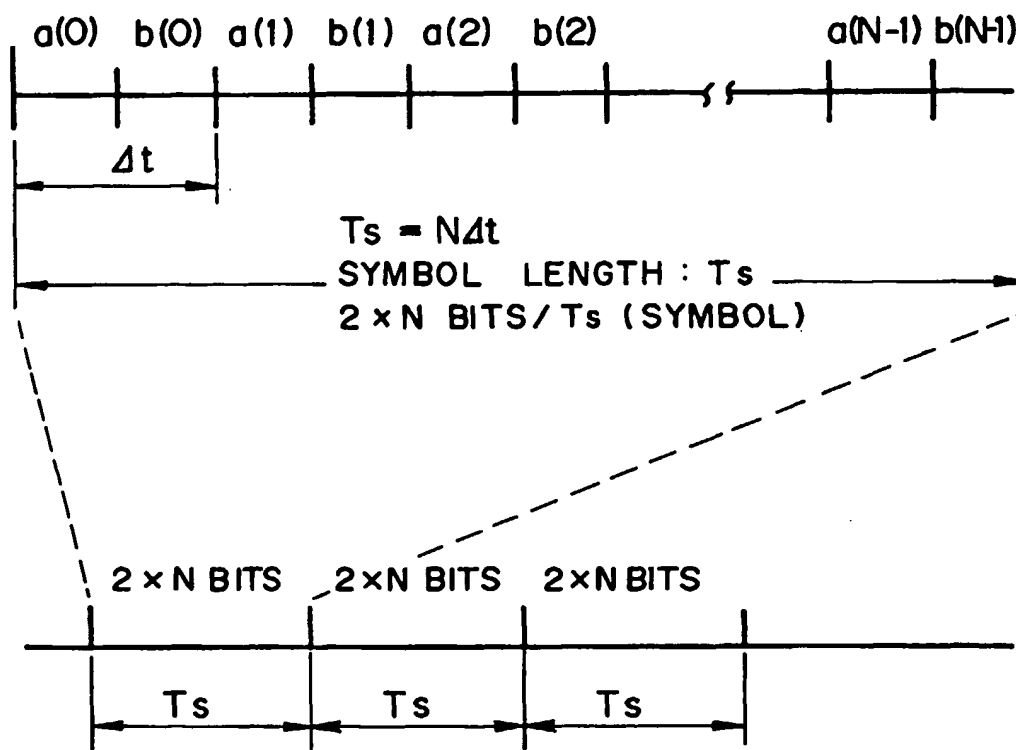


FIG. 16

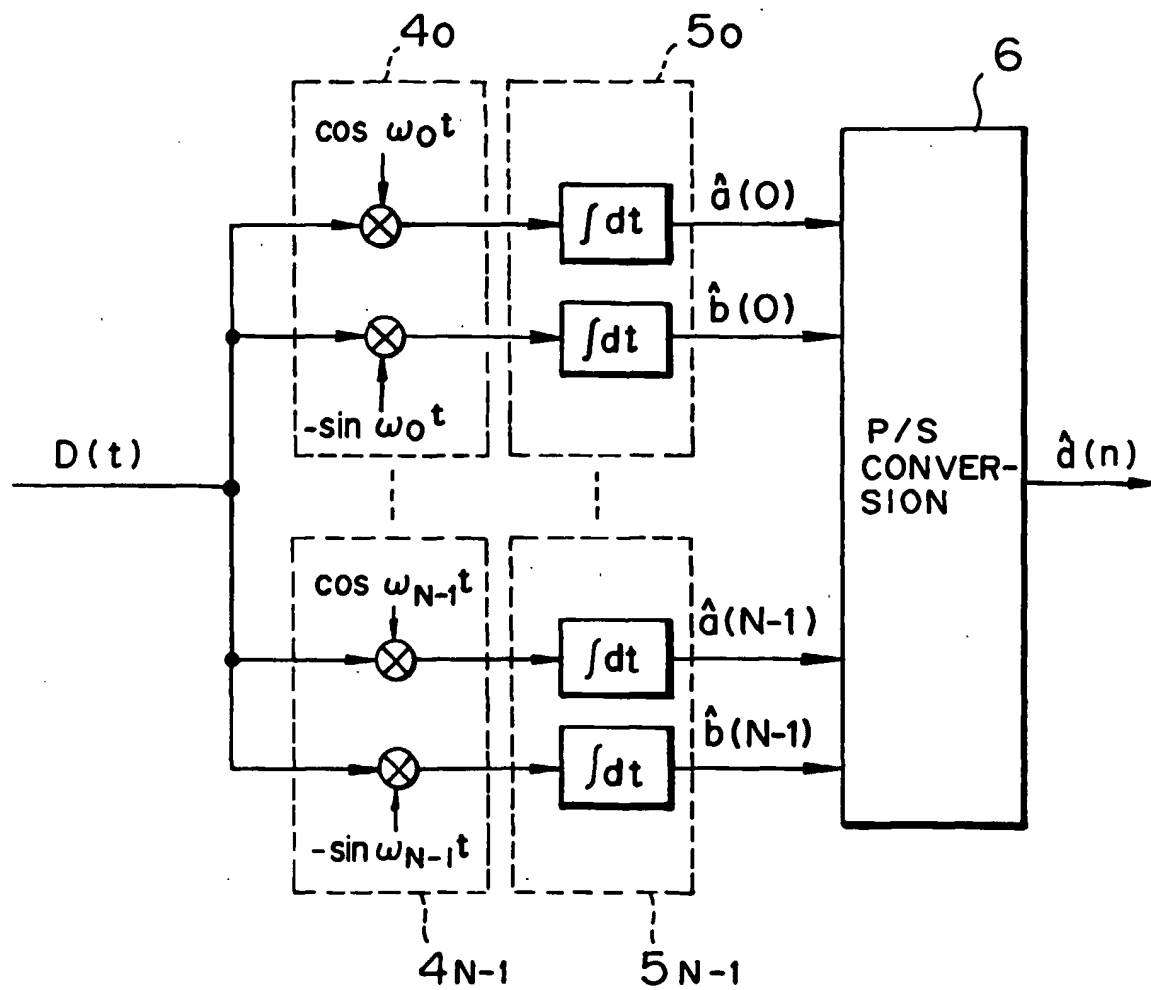


FIG. 17

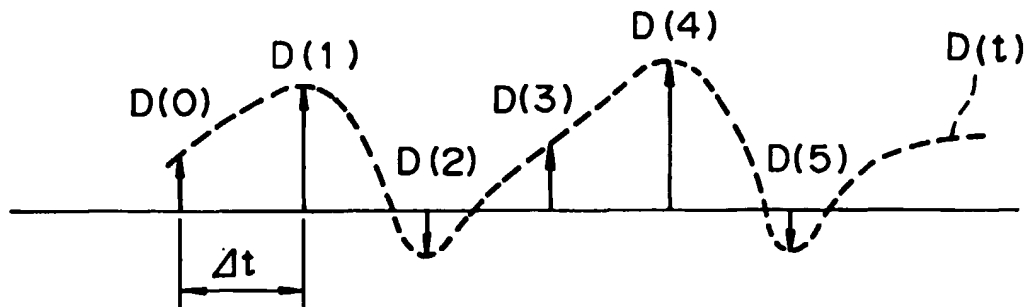


FIG. 18A

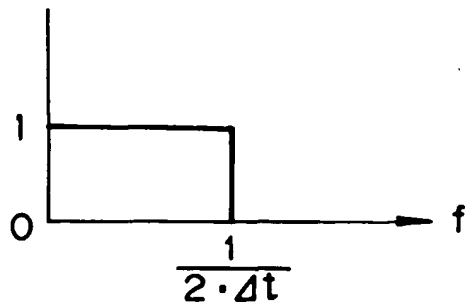


FIG. 18B

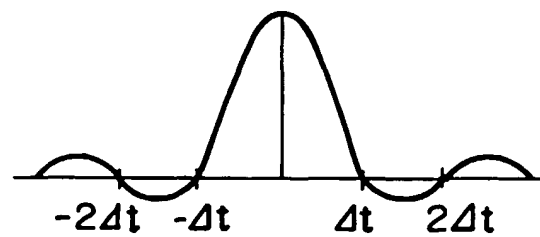


FIG. 19

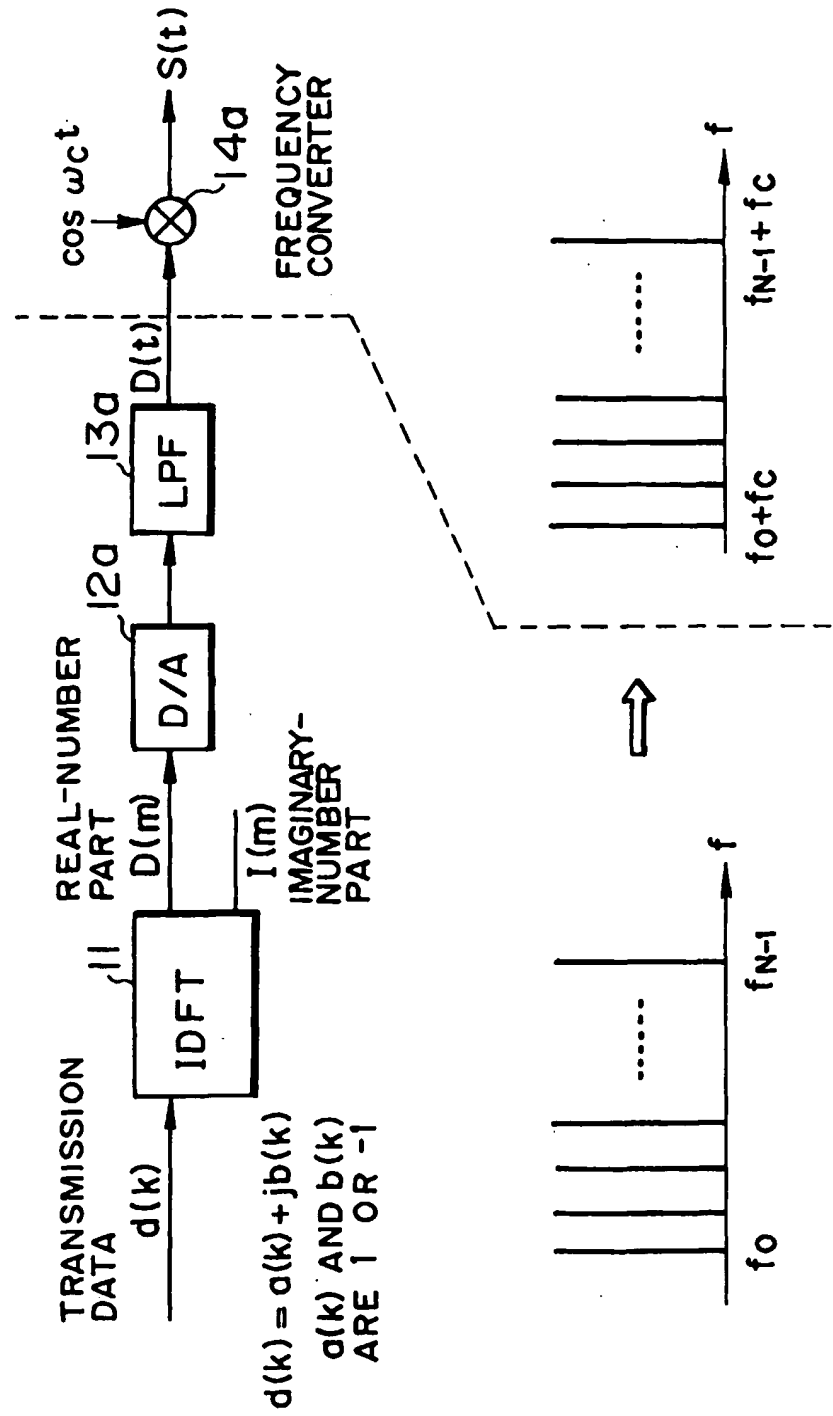




FIG. 20A

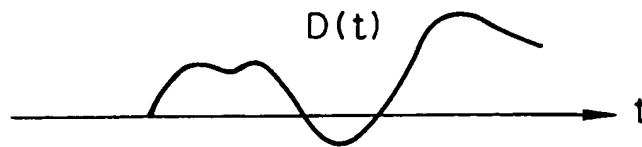


FIG. 20B

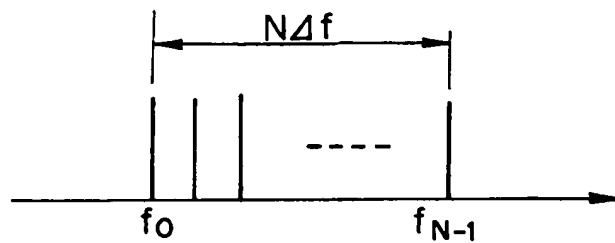


FIG. 21

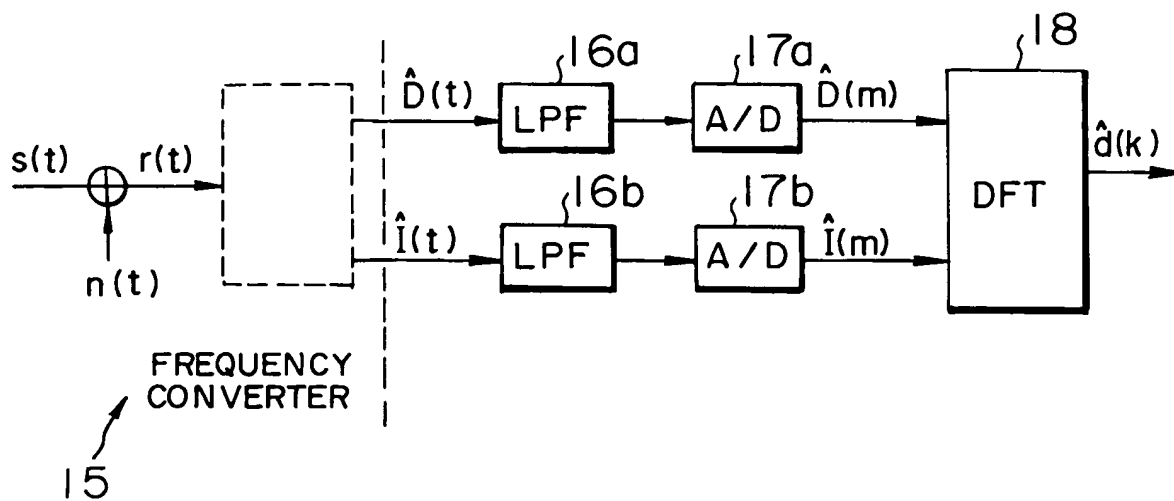


FIG. 22

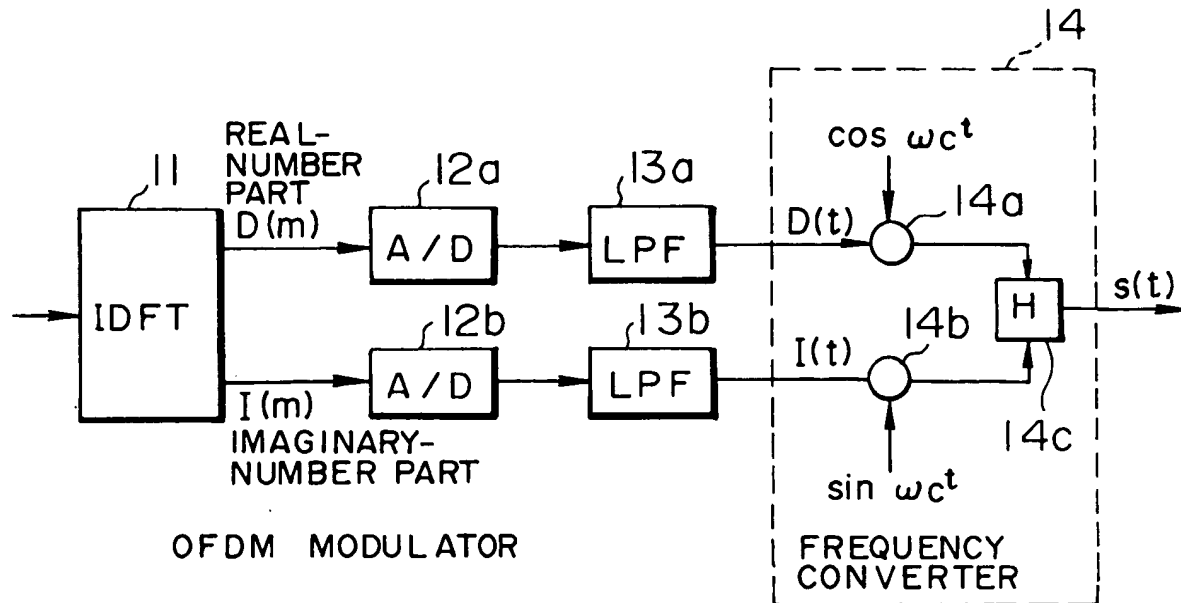


FIG. 23

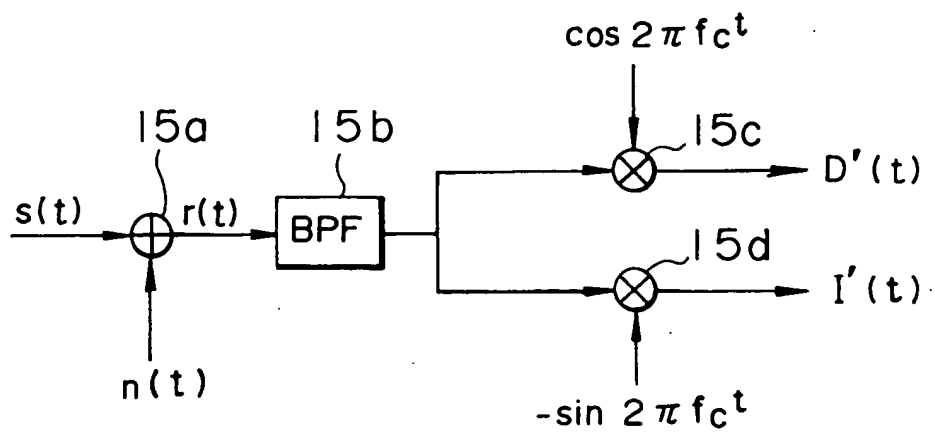


FIG. 24

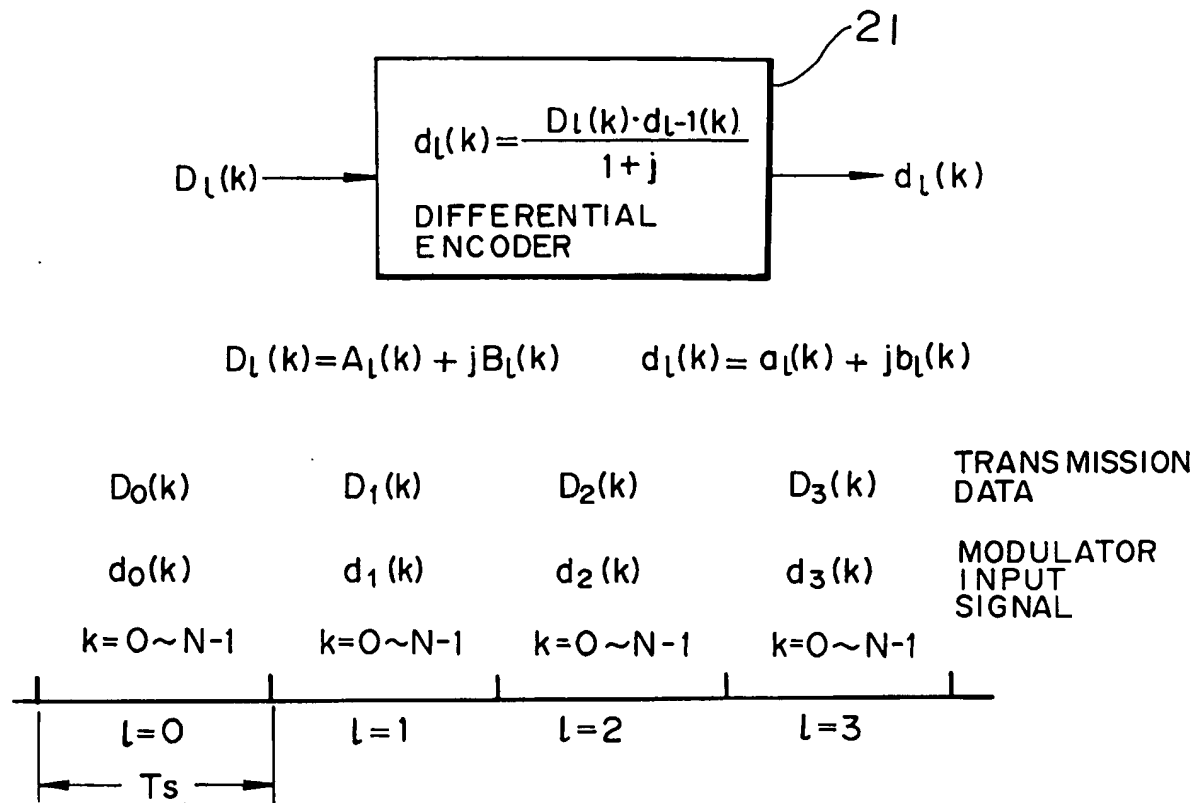


FIG. 25

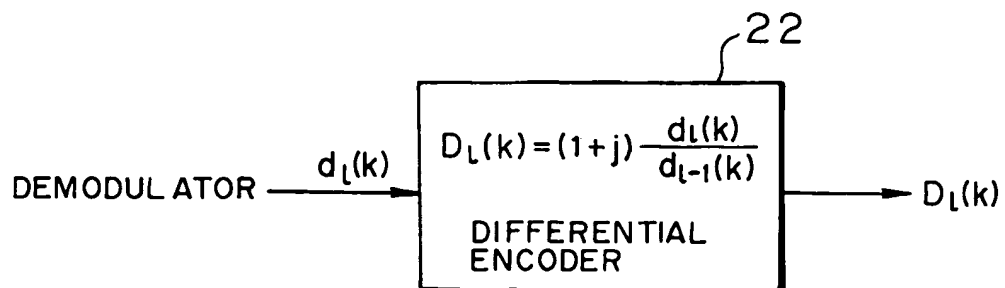


FIG. 26A

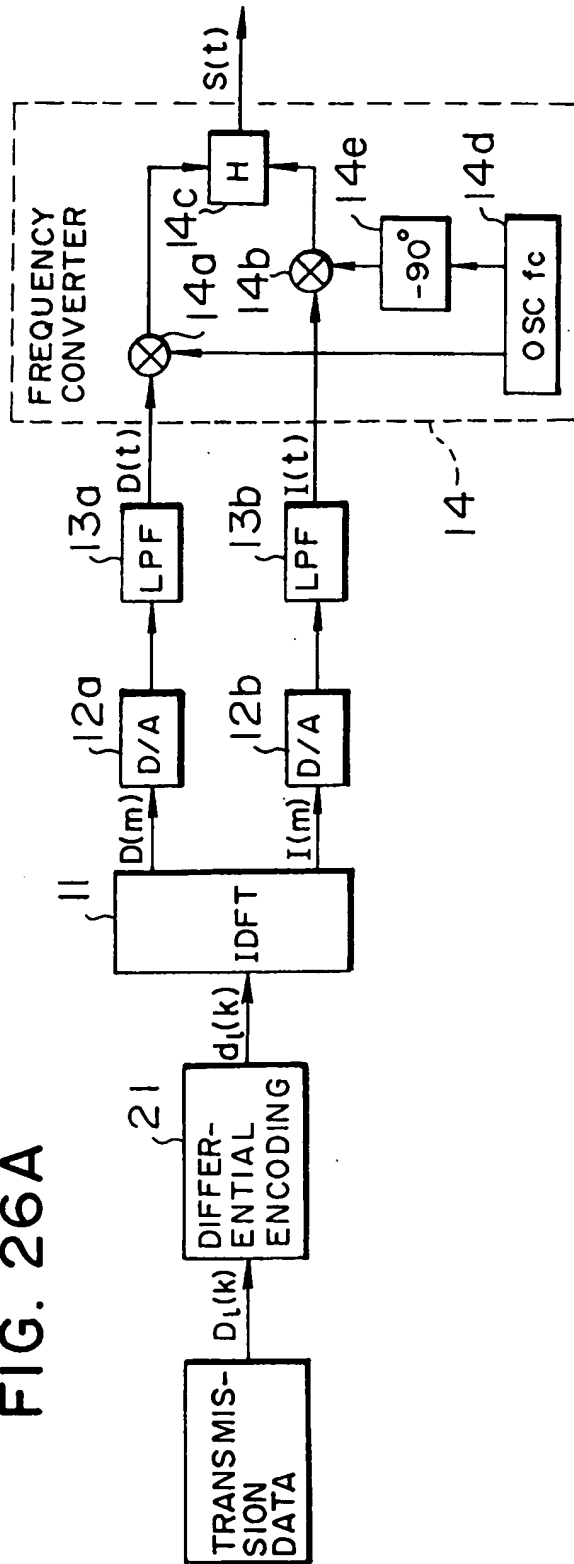


FIG. 26B

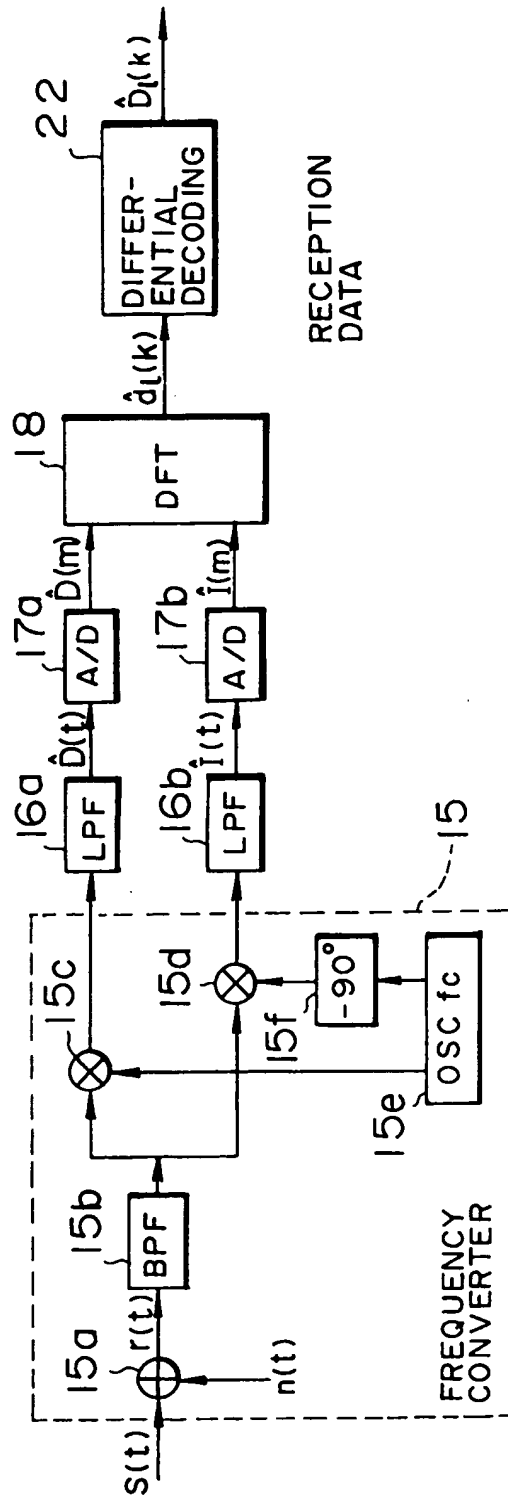


FIG. 27

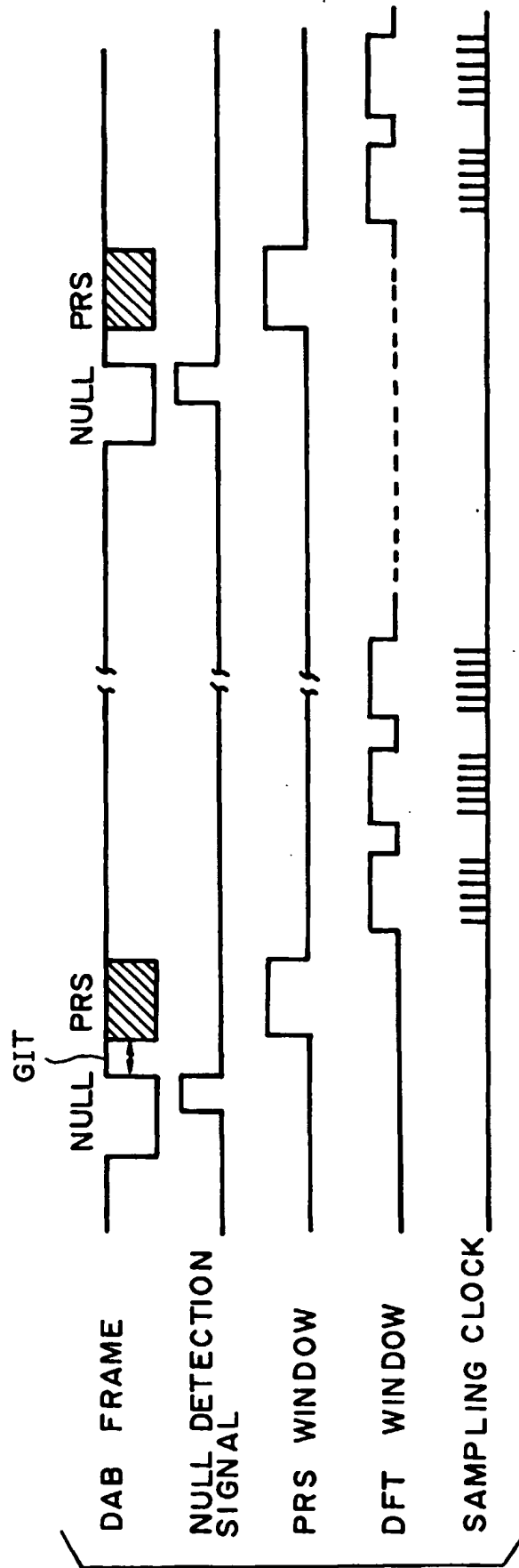
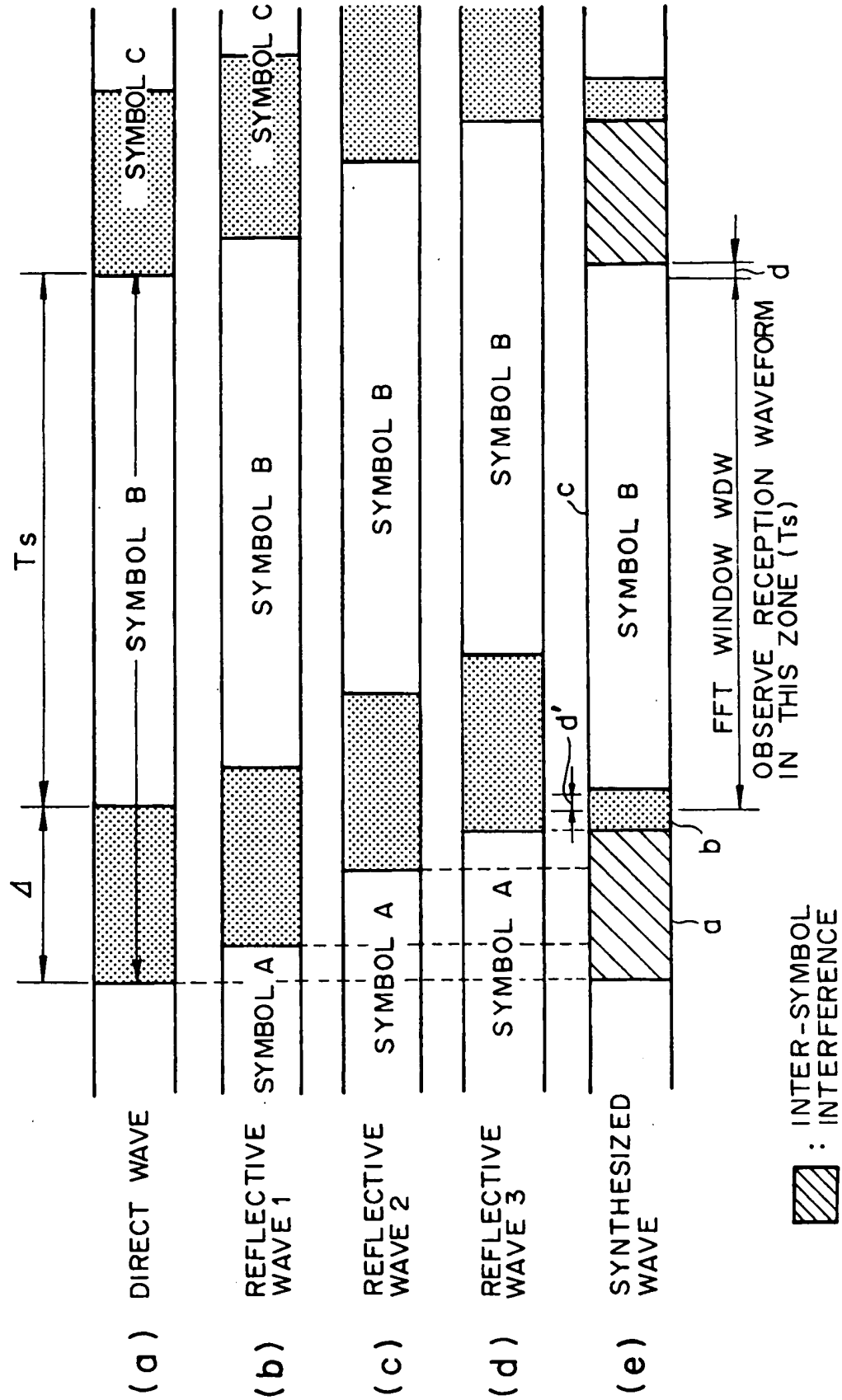


FIG. 28



(19)



Europäisches Patentamt

European Patent Office

Office européen des brevets



(11)

EP 0 837 582 A3

(12)

## EUROPEAN PATENT APPLICATION

(88) Date of publication A3:  
22.08.2001 Bulletin 2001/34

(51) Int Cl.7: H04L 27/26

(43) Date of publication A2:  
22.04.1998 Bulletin 1998/17

(21) Application number: 97117972.6

(22) Date of filing: 16.10.1997

(84) Designated Contracting States:  
AT BE CH DE DK ES FI FR GB GR IE IT LI LU MC  
NL PT SE  
Designated Extension States:  
AL LT LV RO SI

(72) Inventor: Nemoto, Hiroyuki  
Iwaki-city, Fukushima (JP)

(74) Representative: Hirsch, Peter, Dipl.-Ing.  
Klunker Schmitt-Nilson Hirsch  
Winzererstrasse 106  
80797 München (DE)

(30) Priority: 18.10.1996 JP 27596896

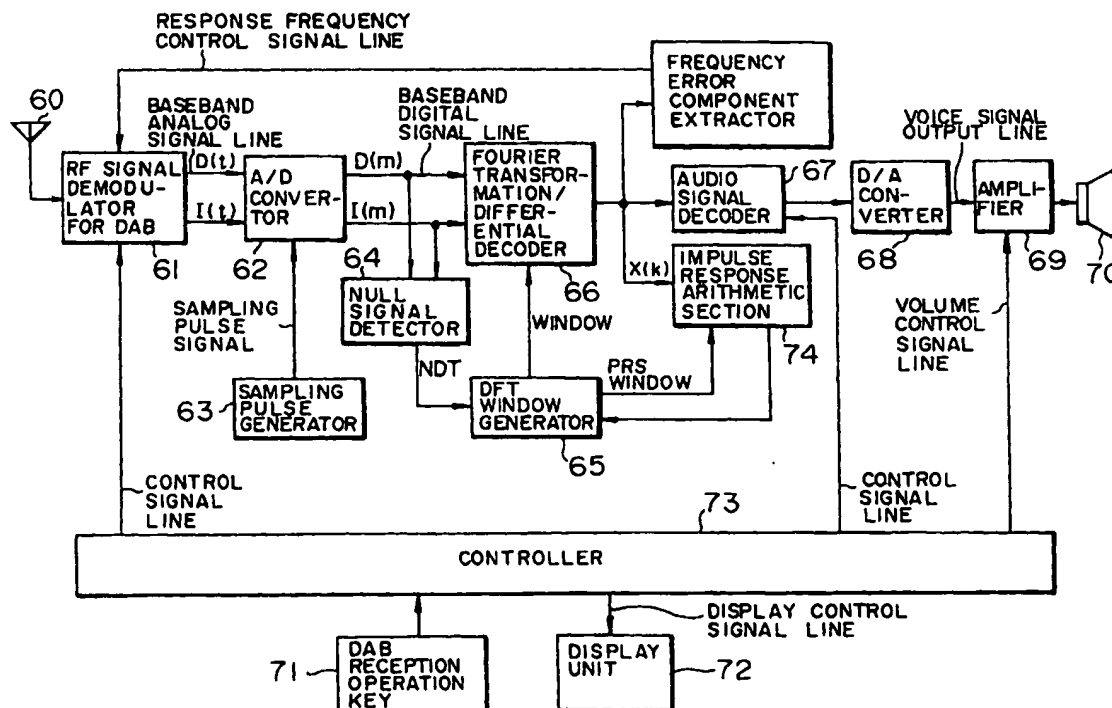
(71) Applicant: Alpine Electronics, Inc.  
Tokyo 141 (JP)

## (54) Symbol synchronization in a DAB receiver

(57) A DFT window generator 65 sequentially shifts the position of a window having a guard interval width  $\Delta$  and calculates the energy of an impulse response in a window at respective positions to obtain a window po-

sition where the maximum energy can be obtained, and the window position where the maximum energy can be obtained is set as the start edge position of the DFT window.

FIG.10





European Patent  
Office

# EUROPEAN SEARCH REPORT

Application Number  
EP 97 11 7972

DOCUMENTS CONSIDERED TO BE RELEVANT			
Category	Citation of document with indication, where appropriate, of relevant passages	Relevant to claim	CLASSIFICATION OF THE APPLICATION (Int.Cl.6)
P,X	WO 97 07620 A (PHILIPS ELECTRONICS NV ;PHILIPS NORDEN AB (SE)) 27 February 1997 (1997-02-27) * page 4, line 14 - page 5, line 29 * * page 6, line 24 - page 7, line 26 * * figure 3 *	1	H04L27/26
P,X	EP 0 829 988 A (NOKIA TECHNOLOGY GMBH) 18 March 1998 (1998-03-18) * column 1, line 9 - column 1, line 29 * * column 6, line 39 - column 8, line 12 * * column 3, line 10 - column 3, line 20 * * figures 5,7 *	1	
A	WO 96 19056 A (LOENROTH BRIAN ;RINGSET VIDAR (NO); HD DIVINE (SE); ROTH GOERAN (S)) 20 June 1996 (1996-06-20) * the whole document *	1-10	
A	US 5 471 464 A (IKEDA YASUNARI) 28 November 1995 (1995-11-28) * column 1, line 7 - column 4, line 39 * * column 8, line 34 - column 8, line 49 *	1-10	
A	WO 96 02989 A (KONLE TILMAR ;WECK CHRISTFRIED (DE)) 1 February 1996 (1996-02-01) * the whole document *	1-10	
A	TOURTIER P J ET AL: "MULTICARRIER MODEM FOR DIGITAL HDTV TERRESTRIAL BROADCASTING", SIGNAL PROCESSING. IMAGE COMMUNICATION,NL,ELSEVIER SCIENCE PUBLISHERS, AMSTERDAM, VOL. 5, NR. 5/06, PAGE(S) 379-403 XP000426711 ISSN: 0923-5965 * Sections 3.4, 3.5, 3.6, 3.8 *	1-10	<div>TECHNICAL FIELDS SEARCHED (Int.Cl.6)</div> <div>H04L H04H</div>
The present search report has been drawn up for all claims			
Place of search MUNICH		Date of completion of the search 26 June 2001	Examiner Palacián Lisa, M
<div>CATEGORY OF CITED DOCUMENTS</div> <div> X : particularly relevant if taken alone  Y : particularly relevant if combined with another document of the same category  A : technological background  O : non-written disclosure  P : intermediate document  T : theory or principle underlying the invention  E : earlier patent document, but published on, or after the filing date  D : document cited in the application  L : document cited for other reasons  &amp; : member of the same patent family, corresponding document </div>			



**ANNEX TO THE EUROPEAN SEARCH REPORT  
ON EUROPEAN PATENT APPLICATION NO.**

EP 97 11 7972

This annex lists the patent family members relating to the patent documents cited in the above-mentioned European search report. The members are as contained in the European Patent Office EDP file on  
The European Patent Office is in no way liable for these particulars which are merely given for the purpose of information.

26-06-2001

Patent document cited in search report		Publication date	Patent family member(s)	Publication date
WO 9707620 A		27-02-1997	CA 2202752 A	27-02-1997
			EP 0786183 A	30-07-1997
			JP 10507616 T	21-07-1998
			US 5848107 A	08-12-1998
<hr/>				
EP 0829988 A		18-03-1998	FI 963649 A	17-03-1998
			US 6125124 A	26-09-2000
<hr/>				
WO 9619056 A		20-06-1996	SE 504787 C	28-04-1997
			AU 4275196 A	03-07-1996
			CN 1170486 A	14-01-1998
			JP 10510958 T	20-10-1998
			SE 9404356 A	15-06-1996
<hr/>				
US 5471464 A	A	28-11-1995	JP 7046217 A	14-02-1995
<hr/>				
WO 9602989 A		01-02-1996	DE 4425713 C	20-04-1995
			AT 170685 T	15-09-1998
			AU 681806 B	04-09-1997
			AU 3162795 A	16-02-1996
			CZ 9603697 A	16-04-1997
			DE 59503453 D	08-10-1998
			DK 771497 T	07-06-1999
			EP 0771497 A	07-05-1997
			ES 2121410 T	16-11-1998
			FI 970204 A	17-01-1997
			HU 77417 A, B	28-04-1998
			JP 2901018 B	02-06-1999
			JP 9512156 T	02-12-1997
			PL 318348 A	09-06-1997
			US 6115354 A	05-09-2000
<hr/>				